

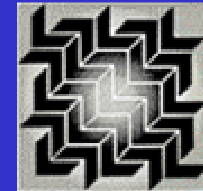
Institute for Pure & Applied Mathematics
An NSF Math Institute at UCLA

Workshop I: Quantum and Atomistic Modeling of Materials Defects October 1 - 5, 2012

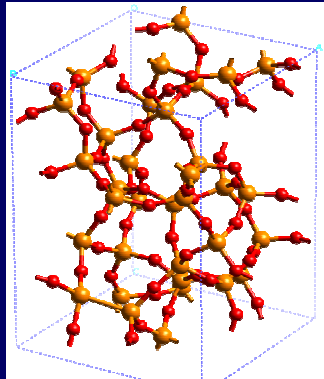
THEORY OF MAGNETIC IMPURITIES IN INSULATING AND SEMICONDUCTING OXIDES. PROBLEMS (AND SOLUTIONS?)



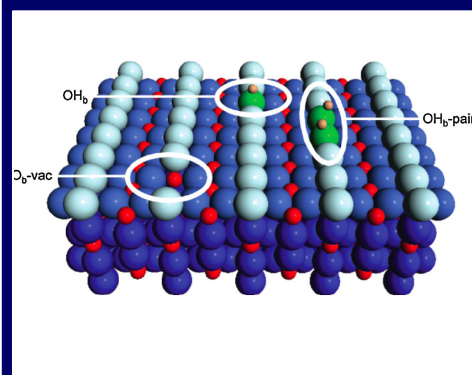
Gianfranco Pacchioni
*Dipartimento di Scienza dei Materiali
Università Milano-Bicocca, Milan (Italy)*



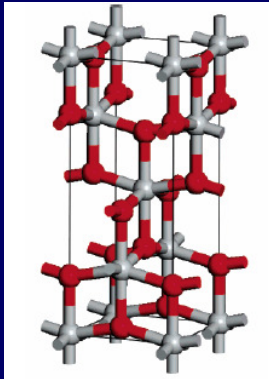
THEORY OF DEFECTS AND DOPANTS IN BULK OXIDES



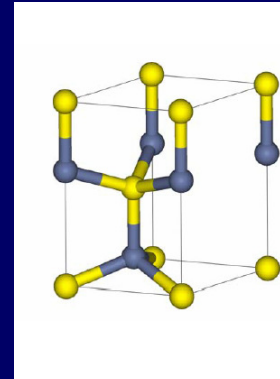
Al:SiO₂



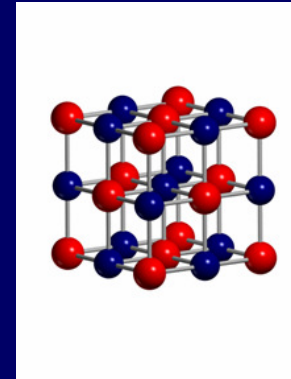
TiO_{2-x}



N:TiO₂



N:ZnO



N:MgO

Common denominator: nature of magnetic impurities

PERIODIC AND CLUSTER MODELS OF SOLIDS AND SURFACES

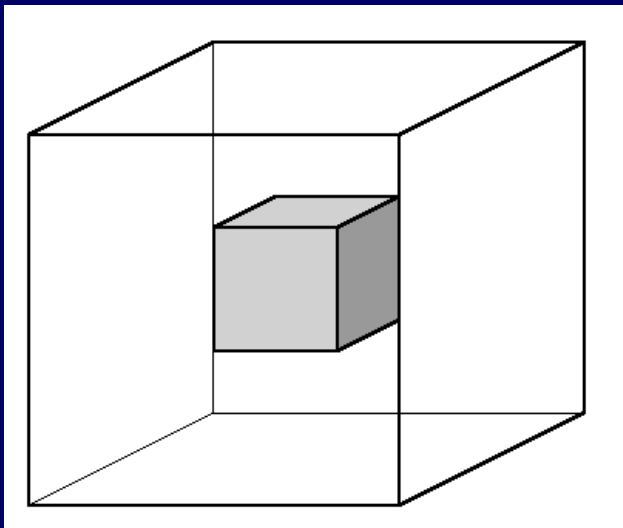
molecular orbitals theory
clusters of atoms

atomic orbitals basis set

solid state effects from embedding

typical cluster size 50 atoms

**models isolated defects or
adsorbates**



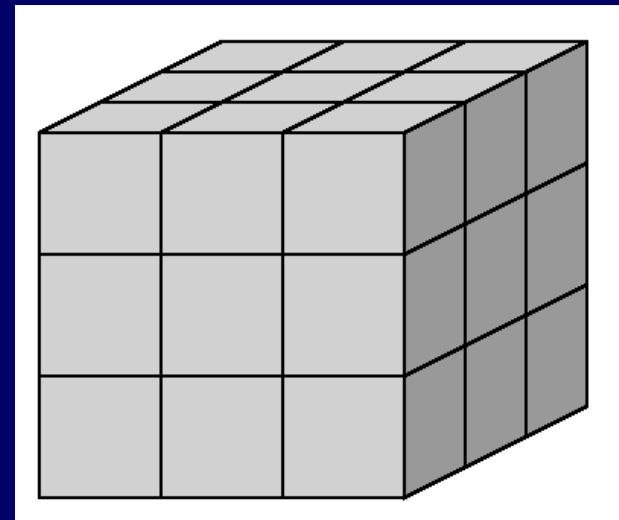
band structure theory
periodic supercell

plane waves basis set

repeated in three-dimensions

typical cell size 100-200 atoms

**models high concentration of
defects or adsorbates**



SPIN LOCALIZATION IN INSULATORS: A CASE STUDY, THE $[\text{AlO}_4]^\circ$ CENTER IN QUARTZ

$[\text{AlO}_4]^\circ$: trivalent Al introduces a hole in the silica lattice

First experimental data go back to 1954....

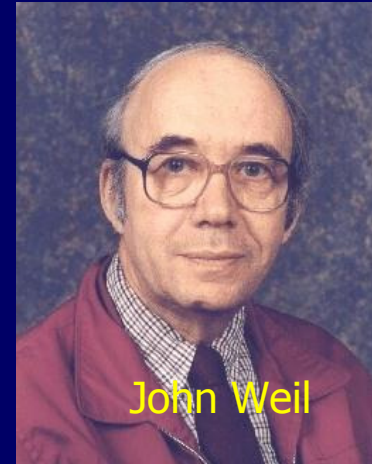
Griffiths et al. Nature, 173, 439 (1954)

First EPR study of irradiated quartz: "the Al atom is at the Si site with the unpaired electron in a localized orbital on one of the nearest O atoms"

O'Brien, Proc. Royal Soc. A231, 404 (1955)

accurate EPR measurements and HF cluster calculations performed in early '80s

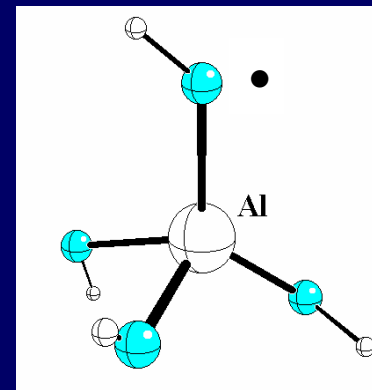
Weil et al. Can. J. Phys. 62, 21 (1984)



John Weil

Hartree-Fock (HF) calculation on $[\text{Al}(\text{OH})_4]^\circ$ cluster

hole localized on one oxygen only



Everything clear? HF has no correlation!

All-electron study of the electronic properties of quartz with Al substitutional impurity

A. Continenza and A. Di Pomponio

Istituto Nazionale di Fisica della Materia (INFN), Dipartimento di Fisica, Università degli studi di L'Aquila, I-67010 Coppito, L'Aquila, Italy

(Received 28 May 1996)

An aluminum defect in quartz has been studied by means of all-electron calculations based on the full-potential linearized-augmented-plane-wave method. A comparative study of alumina, pure quartz, and Al-substituted quartz shows that the Al impurity introduces levels between the bonding and nonbonding states of pure SiO_2 α quartz; these features are shown to derive from the formation of the Al-O chemical bond. The dangling bond in the $[\text{Al}(\text{O}_4)_{1/2}]^-$ unit is evenly shared among the four oxygen atoms adjacent to the defect, and no bias of the charge density around the impurity is observed. A planar averaged potential energy curve for a light carrier ion (e.g., Li^+ , H^+), trapped in an optical channel of the defective quartz has been determined as a function of its location with respect to the aluminum position. [S0163-1829(96)01243-X]

B. Dangling bond around the Al site and the average potential curve

As discussed in Sec. III A, the charge depletion around Al atomic site is due to the reduced valence of the substitutional impurity with respect to the silicon atoms: this results in a dangling bond located in the $[\text{Al}(\text{O}_4)_{1/2}]^-$ unit. An accurate analysis of the charge density around the defect shows that the dangling bond is evenly shared among the four oxygen atoms close to the Al impurity. This can be deduced by the electronic charge deformation map, i.e., the difference between the charge densities of the defective and pure solid, projected in the corresponding bonding planes. In Fig. 7 we

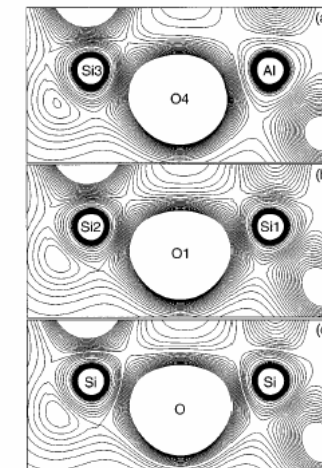


FIG. 5. Valence charge density of $\text{Si}_{16}\text{Al}_{16}\text{O}_{32}$ system [panels (a) and (b)], and α quartz (c), projected in the Al-O4-Si3, Si1-O1-Si2 and Si-O-Si bonding planes, respectively. Lines of equal value are separated by $5e/V_q$, where V_q is the volume of the α -quartz unit cell.

Microscopic structure of the substitutional Al defect in α quartz

Marco Magagnini and Paolo Giannozzi

Scuola Normale Superiore, Piazza dei Cavalieri 7, I-56126 Pisa, Italy

and Istituto Nazionale per la Fisica della Materia (INFN), Corso Perrone 24, I-16152 Genova, Italy

Andrea Dal Corso

SISSA-ISAS, Via Beirut 2/4, I-34014 Trieste, Italy

and Istituto Nazionale per la Fisica della Materia (INFN), Corso Perrone 24, I-16152 Genova, Italy

(Received 16 July 1999)

First-principles pseudopotential calculations are reported for the lattice distortion and electronic properties of the Al substitutional defect in α quartz. We determine microscopical properties of the center such as Al coordination, symmetry of the distorted lattice and defect-induced electronic states. The localization properties of the electronic spin density of this paramagnetic color center are investigated. Our results show that the spin density is evenly distributed on the four oxygen nearest neighbors to Al in contrast to phenomenological model results.

C. Localization of spin density

The localization and symmetry properties of the spin density of the Al- h center are important for interpreting EPR data. Until now these data have been interpreted using a phenomenological model in which the hole was supposed to be located on one oxygen $2p$ antibonding orbital and to oscillate between two oxygens because of thermal motion.^{1,2} Our results do not support this model: the calculated spin density in the ground electronic state, depicted in Fig. 7, is localized in antibonding $2p$ oxygen orbitals but is evenly distributed on *all* the four oxygens. Comparison of the spin

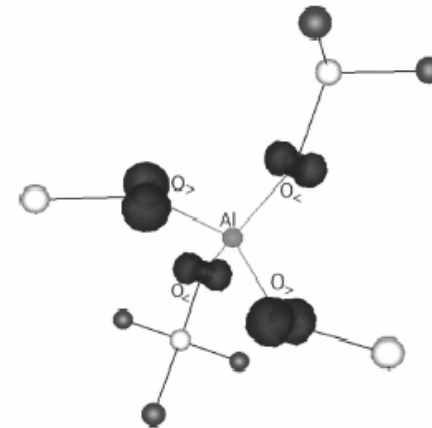


FIG. 7. Calculated spin density for the Al- h center. Surface of constant value equal to 0.02 (a.u.)^{-3} (1/4 of the maximum value). Oxygen ions are dark grey and Si ions are white.

Local chemistry of Al and P impurities in silica

J. Lægsgaard

Research Center COM, Technical University of Denmark, Building 349, DK-2800 Lyngby, Denmark

K. Stokbro

Mikroelektronik Centret, Technical University of Denmark, Building 345 East, DK-2800 Lyngby, Denmark

(Received 21 December 1999)

The local structure around Al and P impurities in silica is investigated using density-functional theory. Two distinct cases are considered: impurities substituting for a Si atom in α quartz, and impurities implanted in a stoichiometric α -quartz crystal. Both impurity elements are found to have similar stable substitutional configurations; however, when they are implanted the geometries are quite different: While P prefers to stay in the interstitial region, Al tends to substitute for a Si atom, which in this way is forced into the interstitial region. The underlying chemical origin of the differences is revealed by an analysis of the electronic impurity levels, and the results clarify previous experimental data.

In conclusion, we have clarified the chemical nature of substitutional and implanted Al and P impurities in α -quartz. Al and P were both found to have stable substitutional configurations, but with some differences in the local structure. While the extra electron in the PO_4 unit is mainly located in two of the bonds that are $\sim 0.05 \text{ \AA}$ longer than the other two, the hole present in the AlO_4 unit is evenly distributed over the four bonds, and the difference between short and long bond lengths is comparable to that in pure quartz. The im-

THE METHODS

Hartree-Fock HF (HF, UHF)

$$E_{\text{HF}} = E_{\text{NUCL}} + \langle hP \rangle + 1/2 \langle PJ(P) \rangle - 1/2 \langle PK(P) \rangle$$

E_{NUCL}

nuclear repulsion energy

P

density matrix

$\langle hP \rangle$

one-electron term

$1/2 \langle PJ(P) \rangle$

classical Coulomb repulsion term

$-1/2 \langle PK(P) \rangle$

exchange energy (exact in HF)

HF: no electron correlation

Correlation effects may be included through CI or MP theory

Kohn-Sham formulation of DFT (LDA, LSDA)

$$E_{\text{KS}} = E_{\text{NUCL}} + \langle hP \rangle + 1/2 \langle PJ(P) \rangle + E_x + E_c$$

$E_x[P]$

exchange functional

$E_c[P]$

correlation functional

HF special case: $E_x[P] = -1/2 \langle PK(P) \rangle$; $E_c = 0$

hybrid functionals: mix HF with DFT exchange (e.g. B3LYP)

HYBRID FUNCTIONALS: B3LYP

Density-functional thermochemistry. III. The role of exact exchange

Axel D. Becke

Department of Chemistry, Queen's University, Kingston, Ontario, Canada K7L 3N6

(Received 30 October 1992; accepted 16 December 1992)

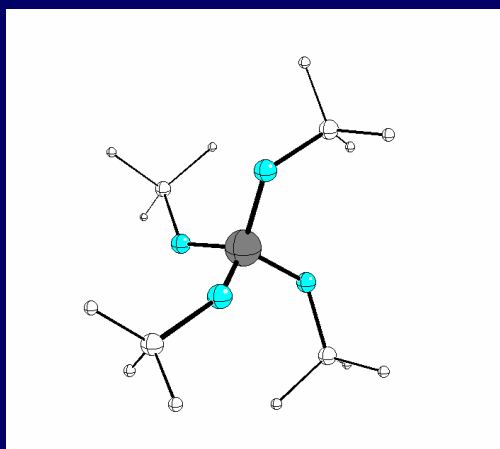
Despite the remarkable thermochemical accuracy of Kohn–Sham density-functional theories with gradient corrections for exchange-correlation [see, for example, A. D. Becke, *J. Chem. Phys.* **96**, 2155 (1992)], we believe that further improvements are unlikely unless *exact-exchange* information is considered. Arguments to support this view are presented, and a semiempirical exchange-correlation functional containing local-spin-density, gradient, and exact-exchange terms is tested on 56 atomization energies, 42 ionization potentials, 8 proton affinities, and 10 total atomic energies of first- and second-row systems. This functional performs significantly better than previous functionals with gradient corrections only, and fits experimental atomization energies with an impressively small average absolute deviation of 2.4 kcal/mol.

$$E_{xc}^{B3LYP} = a E_x^{LSDA} + (1 - a) E_x^{HF} + b \Delta E_x^{Becke} + (1 - c) E_c^{LSDA} + c E_c^{LYP}$$

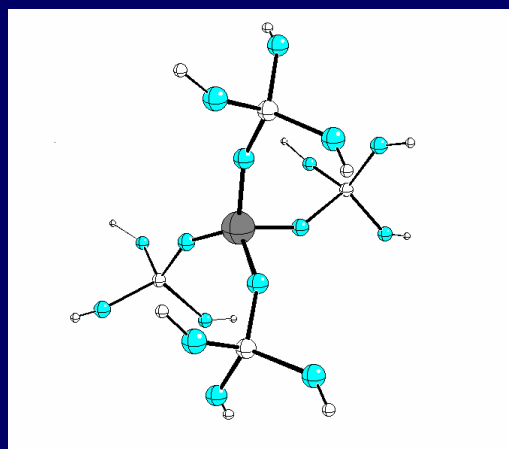
5648 J. Chem. Phys. **98** (7), 1 April 1993

36700 citations!

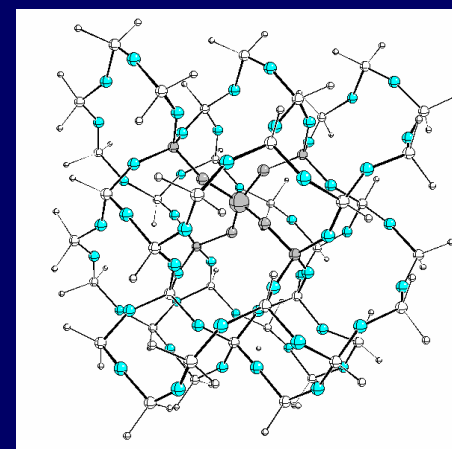
CLUSTER MODELS OF $[\text{AlO}_4]^{0}$ CENTER: HF AND MP2



$\text{Al}(\text{OSiH}_3)_4$



$\text{Al}[\text{OSi}(\text{OH}_3)]_4$



$\text{AlO}_{60}\text{Si}_{44}\text{H}_{60}$

Cluster	spin	HF	MP2
$\text{Al}(\text{OSiH}_3)_4$	O_1	1.04	1.01
	$\text{O}_{2,3,4}$	<0.01	<0.01
$\text{Al}[\text{OSi}(\text{OH}_3)]_4$	O_1	1.04	1.03
	$\text{O}_{2,3,4}$	<0.01	<0.01
$\text{AlO}_{60}\text{Si}_{44}\text{H}_{60}$ (QM-MM)	O_1	1.04	-
	$\text{O}_{2,3,4}$	<0.01	-

■ spin distribution does not depend on cluster size

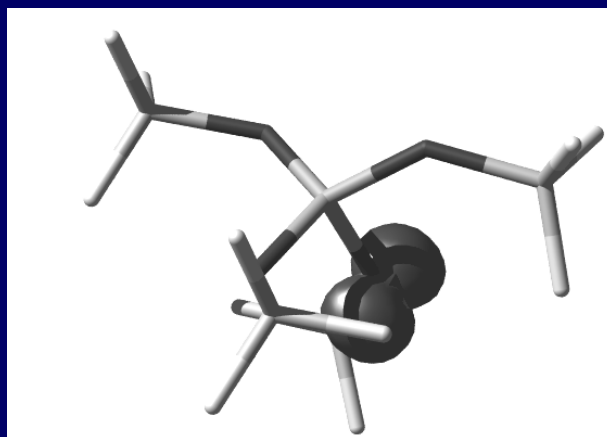
■ spin entirely localized on a single O atom

■ not due to lack of correlation: MP2 gives same spin distribution as HF

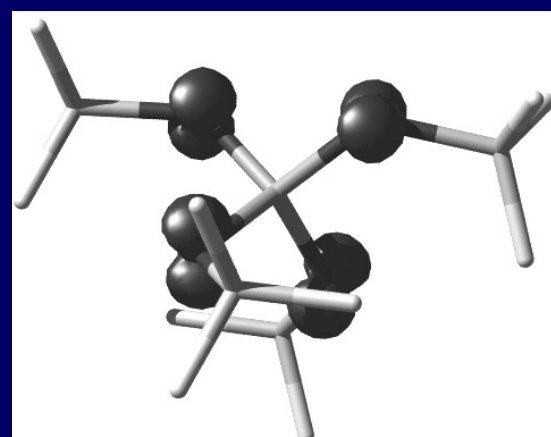
CLUSTER MODELS OF $[\text{AlO}_4]^{0-}$ CENTER: DFT

Physical picture in DFT completely different, spin equally distributed over four O atoms (as reported in PRB papers)

Same result obtained with ALL exchange-correlation functionals (PW91, B3LYP)



HF



DFT

WHERE IS THE TRUE ?

EPR SPECTROSCOPY

Free electron g factor, g_e

Spin-field hamiltonian: $\hat{H} = g_e \frac{\mu_B}{h} \hat{S}_z \cdot B_0$

$$\mathbf{g}\text{-tensor} \Rightarrow \mathbf{g} = \begin{bmatrix} g_1 & 0 & 0 \\ 0 & g_2 & 0 \\ 0 & 0 & g_3 \end{bmatrix}$$

Hyperfine coupling constants (hfcc)

Hamiltonian of hyperfine interaction:

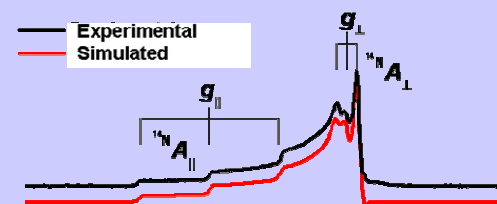
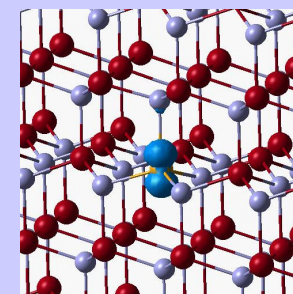
$$\hat{H} = \mathbf{A} \cdot \hat{I}_z \cdot \hat{S}_z$$

\mathbf{A} tensor \Rightarrow interaction of electron spin with nuclear spin

$$\mathbf{A} = \begin{bmatrix} A_1 & 0 & 0 \\ 0 & A_2 & 0 \\ 0 & 0 & A_3 \end{bmatrix} = a_{\text{iso}} \mathbf{U} + \begin{bmatrix} B_1 & 0 & 0 \\ 0 & B_2 & 0 \\ 0 & 0 & B_3 \end{bmatrix}$$

a_{iso} Fermi contact term
(isotropic part)

B_i dipolar interaction



Spin-orbit perturbation approach
Neese, J. Chem. Phys. 115, 11080
(2001)

COMPUTED HYPERFINE COUPLINGS: HF, DFT, EXPERIMENT

^{17}O , G	B3LYP	HF	Exp.
a_{iso}	-4	-36	-26
B_1	12	47	41
B_2	12	48	44
B_3	-25	-95	-85

^{27}Al , G	B3LYP	HF	Exp.
a_{iso}	-11	-5	-6
B_1	0	0	0
B_2	0	0	0
B_3	0	1	1

■ not only O hyperfine but also superhyperfine (Al) interaction reproduced quantitatively in Hartree-Fock

■ unpaired electron: 2% O_{2s} 98% O_{2p} character

■ EPR analysis of ^{17}O hfcc shows that the hole is localized on a single oxygen atom

O Nuttal and Weil, Solid State Commun. 35, 789 (1980); Can. J. Phys. 59, 1696 (1981)

HF PROVIDES THE CORRECT PHYSICAL PICTURE, DFT NOT !

GP, Frigoli, Ricci, Weil, "On the theoretical description of hole localization in a quartz Al centre: the importance of exact exchange", *Physical Review B*, **63**, 054102 (2001)

WHAT WE LEARNED FROM THIS STORY...

failure of DFT due to self-interaction problem; HF energy contains no self-interaction contributions

in DFT unpaired electrons tend to delocalize to reduce Coulomb repulsion

care is necessary when using standard DFT for localized holes

compute observable properties before to conclude about validity of a physical model

Al-DOPED SiO₂: A CLASSICAL CASE TO TEST NEW APPROACHES

Hole localization in al doped silica: A DFT+U description

Nolan, Michael; Watson, Graeme W.

J. CHEMICAL PHYSICS 125, 144701, 2006

Density functional theory description of hole-trapping in SiO₂: A self-interaction-corrected approach

d'Avezac, M; Calandra, M; Mauri, F

PHYSICAL REVIEW B, 71, 205210, 2005

Hole localization in [AlO₄](0) defects in silica materials

To, J; Sokol, AA; French, SA; et al.

J. CHEMICAL PHYSICS, 122, 144704, 2005

Electron hole formation in acidic zeolite catalysts

Solans-Monfort, X; Branchadell, V; Sodupe, M; et al.

J. CHEMICAL PHYSICS, 121, 6034-6041, 2004

Quantum chemical modeling of photoabsorption and photoluminescence of the [AlO₄](0) defect in bulk SiO₂

Zyubin, AS; Mebel, AM; Lin, SH

J. CHEMICAL PHYSICS, 119, 11408-11414, 2003

TiO₂ photoactivity: first study in 1921

Titania particles used for exterior paints since a century

1920: titania-based paints undergo "chalking" in strong sunlight (non-adherent white powder forms on the surface)

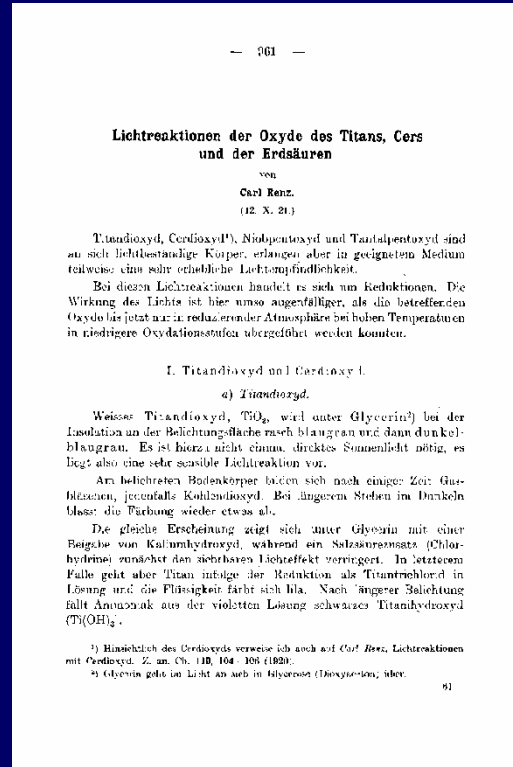
Light destroys the organic component of the paint, leaving the titania exposed



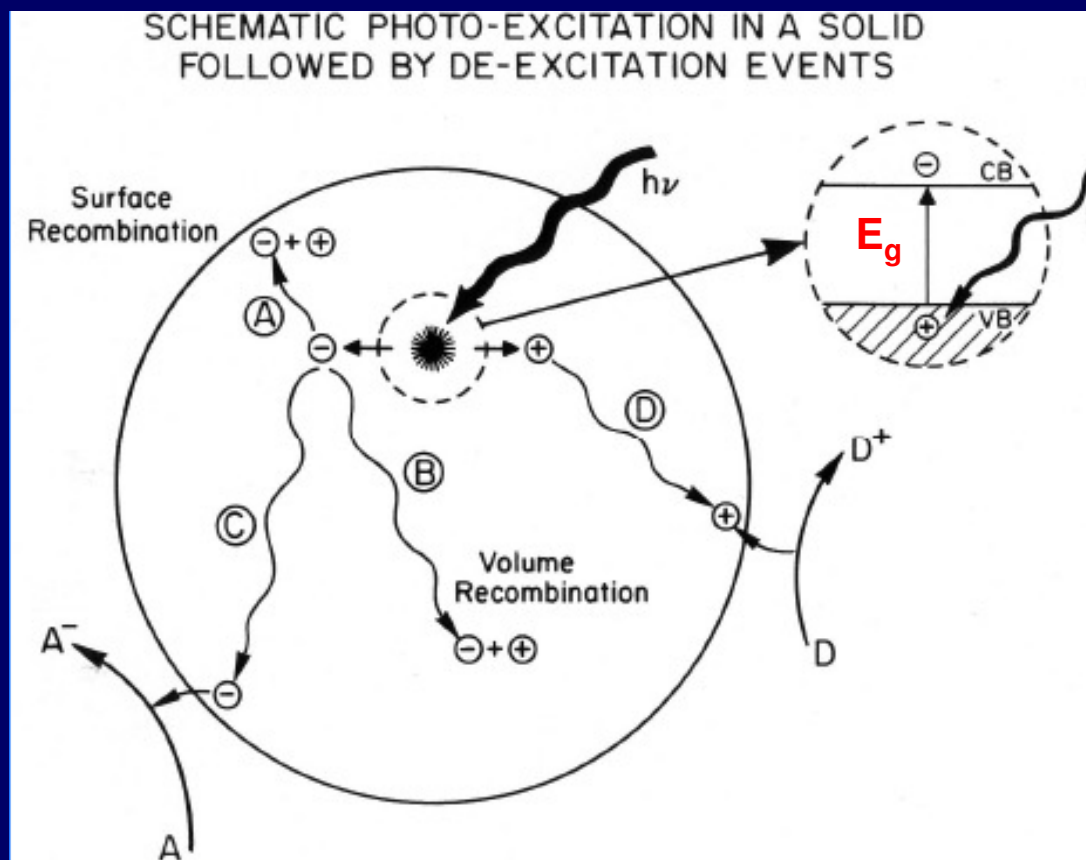
1921: first report of interaction of TiO₂ with light (titania is partially reduced under sunlight in the presence of an organic compound):



C. Renz, *Helv. Chim. Acta* 4 (1921) 961



Photoactivity: the mechanism



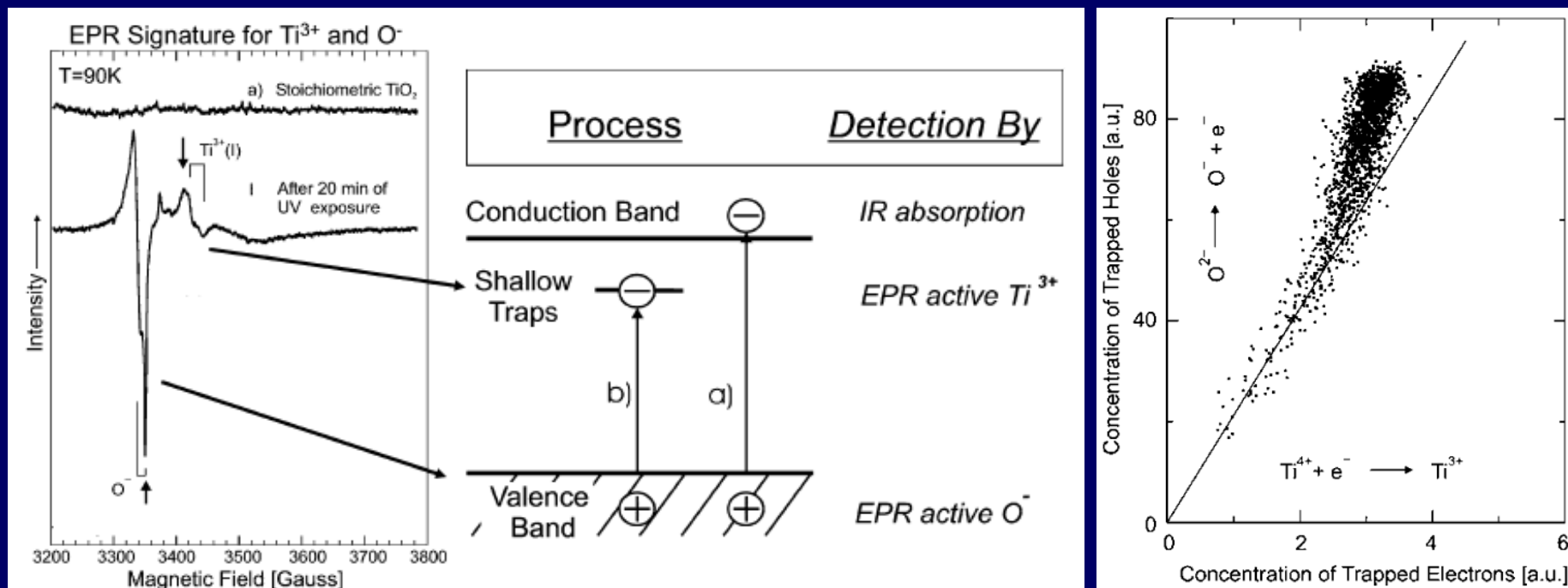
Solar light: a continuous source of energy

Photons are absorbed by the semiconducting material where they generate electrons and holes

Electrons and holes migrate at the surface of the nanoparticle where they react with adsorbed molecules

- (A) Electron and hole migrate to the particle and recombine
- (B) Electron and hole diffuse and recombine in the bulk
- (C) Electrons migrate to the surface where they reduce adsorbed molecules
- (D) Holes migrate to the surface where they oxidize adsorbed molecules

Paramagnetic centers generated by photoexcitation



Left: At low T electrons are trapped at Ti^{4+} sites (formation of Ti^{3+}); holes (+) are trapped at oxide ions (O^-). Lifetime: hours at 90 K.

Right: correlation between photogenerated electrons and holes (from EPR). Deviation from linearity due to electrons transferred to EPR-silent conduction band

Ti^{3+} : a key species in photoactivity of TiO_2 !

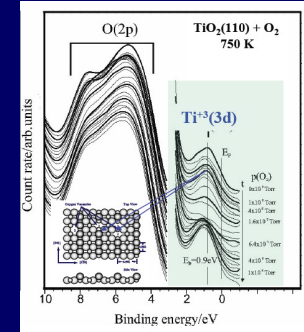
Berger et al. J. Phys. Chem. B 109 (2005) 6061

Experimental proofs of formation of reduced bulk titania (Ti^{3+}):

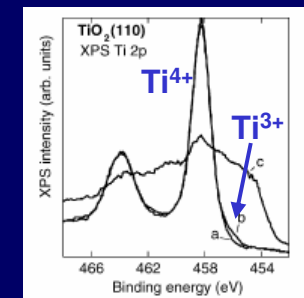
- (1) UPS
- (2) XPS
- (3) EPR
- (4) UV-vis

Every theoretical method dealing with reduced TiO_2 should be able to reproduce these features...

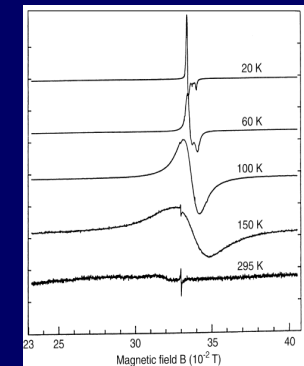
(1) occurrence of a new state in the gap at about 0.8 eV below the conduction band attributed to the reduced Ti^{3+} ions



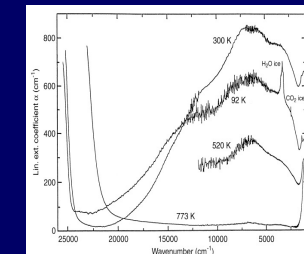
(2) shift in the core level binding energies of the reduced Ti atoms from X-ray photoemission (XPS)



(3) presence of more than one EPR signal associated to various kinds of paramagnetic Ti^{3+} ions in the lattice

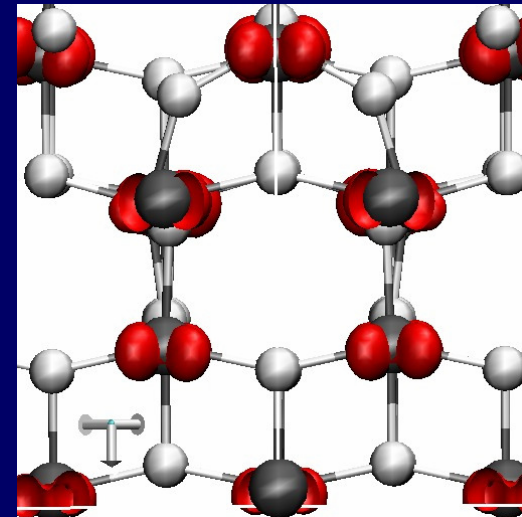
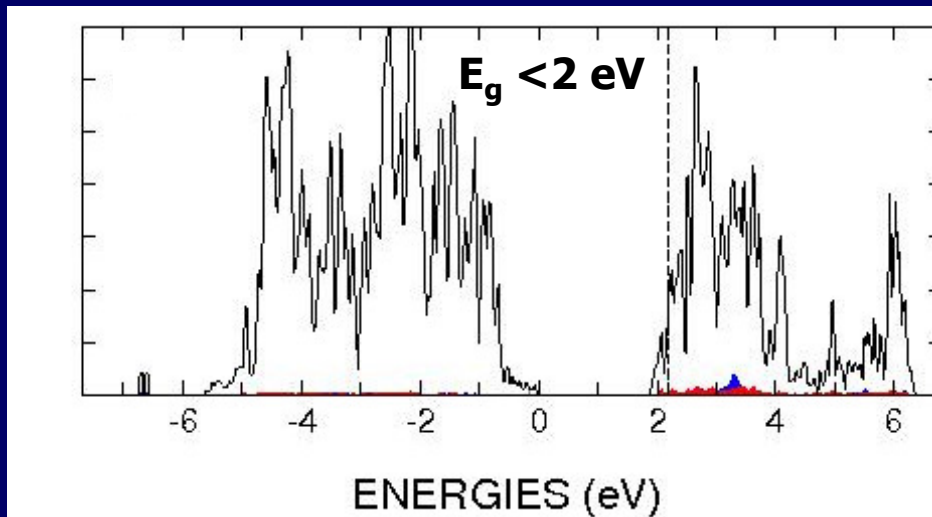


(4) absorption bands in the visible region responsible for the change in color (assigned to d-d transitions)



O VACANCY ON BULK TiO_{2-x}

STANDARD DFT (LDA, GGA)



Band gap is too small; no states in the gap, electrons fully delocalized. Problem due to self-interaction in DFT

BEYOND THE PURE DFT APPROACH

Hybrid functionals

HF-like exchange mixed in with the DFT exchange: B3LYP (20%), H&HLYP (50%)

$$E_{xc}^{B3LYP} = a E_x^{LSDA} + (1 - a) E_x^{HF} + b \Delta E_x^{Becke} + (1 - c) E_c^{LSDA} + c E_c^{LYP}$$

Becke J. Chem. Phys. 98, 5648 (1993)

DFT+U methods

explicit description of correlation by on-site correlation term U for selected localized orbitals. Add a Hubbard-like E_{Hub} term to standard functional:

$$E_{LDA+U}[n(\mathbf{r})] = E_{LDA}[n(\mathbf{r})] + E_{Hub}[\{n_m^{I\sigma}\}] - E_{DC}[\{n^{I\sigma}\}]$$

Anisimov et al., Phys. Rev. B 44, 943 (1991)



1988-2009, University of Torino

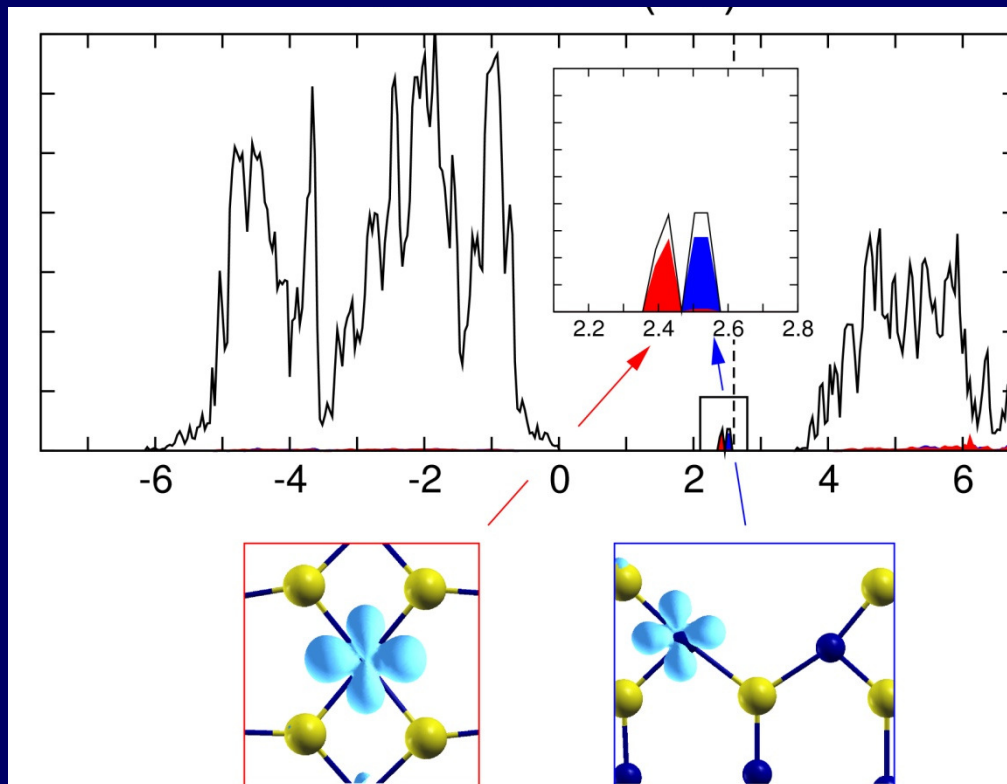
band structure theory

periodic supercell

Atomic orbital basis set

Efficient for hybrid DFT (B3LYP)

O vacancy on rutile (110) surface: hybrid DFT



- O vacancy: two electrons localized on two non-equivalent Ti_{5c} ions
- triplet ground state (magnetic)
- Two states in the gap at 1.2 and 0.9 eV below conduction band (as in the experiment)

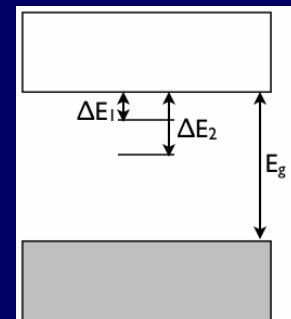
Di Valentin, GP, Selloni, Phys. Rev. Lett. 97, 166803 (2006)

O vacancy in bulk anatase: B3LYP and DFT+U

Remove an O atom: $2e^-$ left on the system

Quantities of interest:

- (1) Energy gap (E_g)
- (2) Distance of impurity levels from bottom of conduction band ($\Delta E_1, \Delta E_2$)

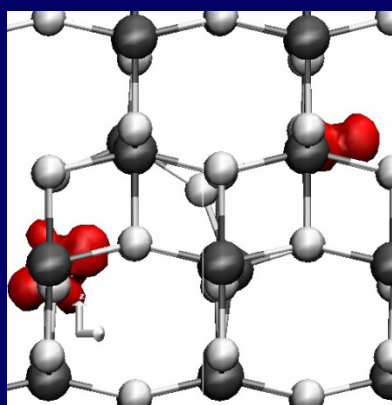
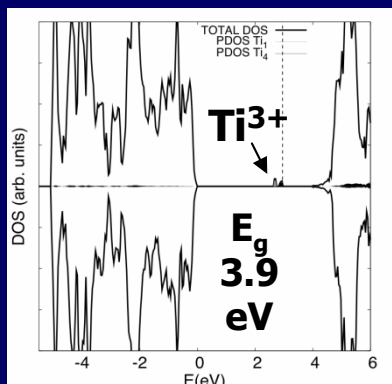


B3LYP

ΔE_1 1.2 eV

ΔE_2 1.3 eV

Both electrons
are localized on
Ti 3d levels ...

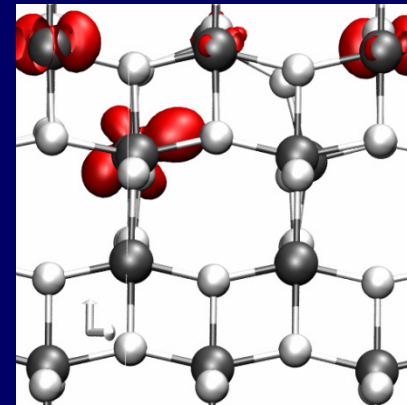
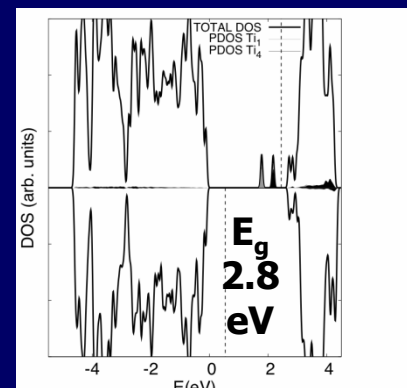


DFT+U (U = 3 eV)

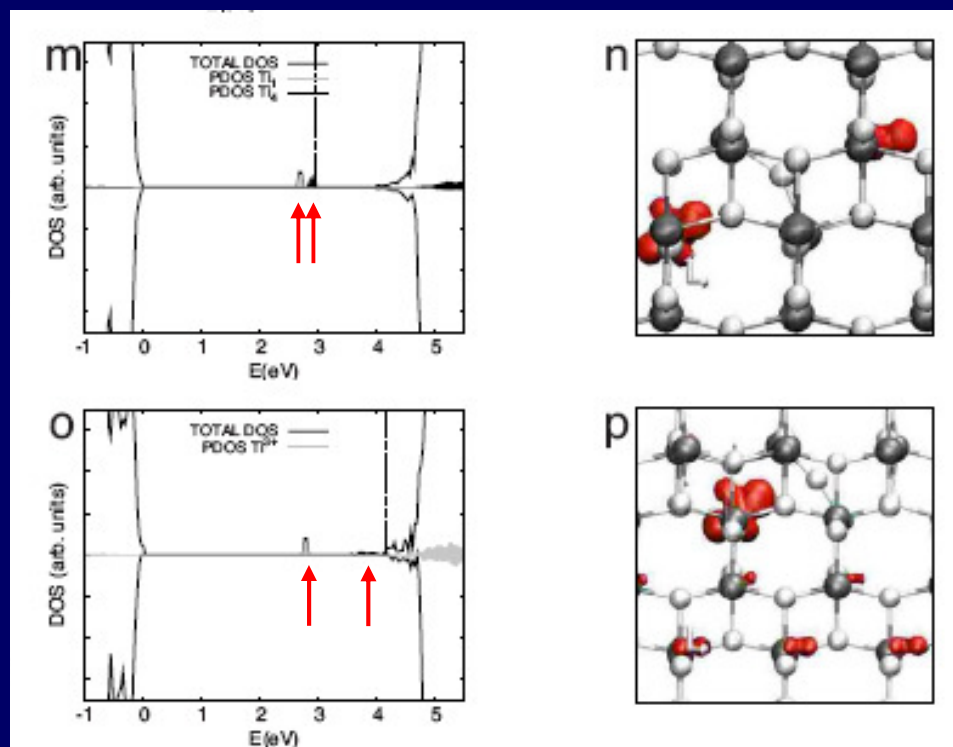
ΔE_1 0.6 eV

ΔE_2 0.9 eV

...but
delocalized
solution is close
in energy



O vacancy in bulk anatase: B3LYP



1st solution: two electrons fully localized on two non-equivalent Ti ions, one undercoordinated and one six-coordinated (ΔE_1 & ΔE_2 1.2-1.3 eV)

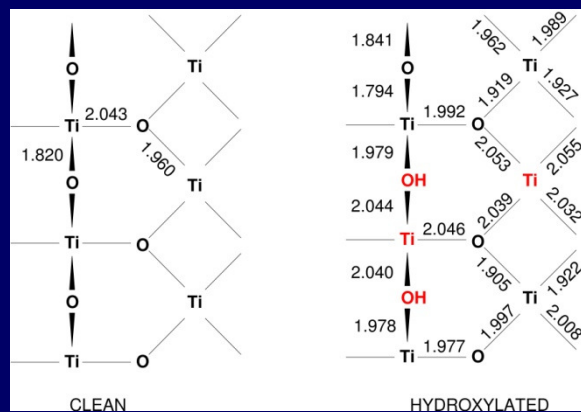
2nd solution: one electron fully localized (ΔE_1 1.5 eV), one is partly delocalized (ΔE_2 0.5 eV)

Energy difference: 60 meV !

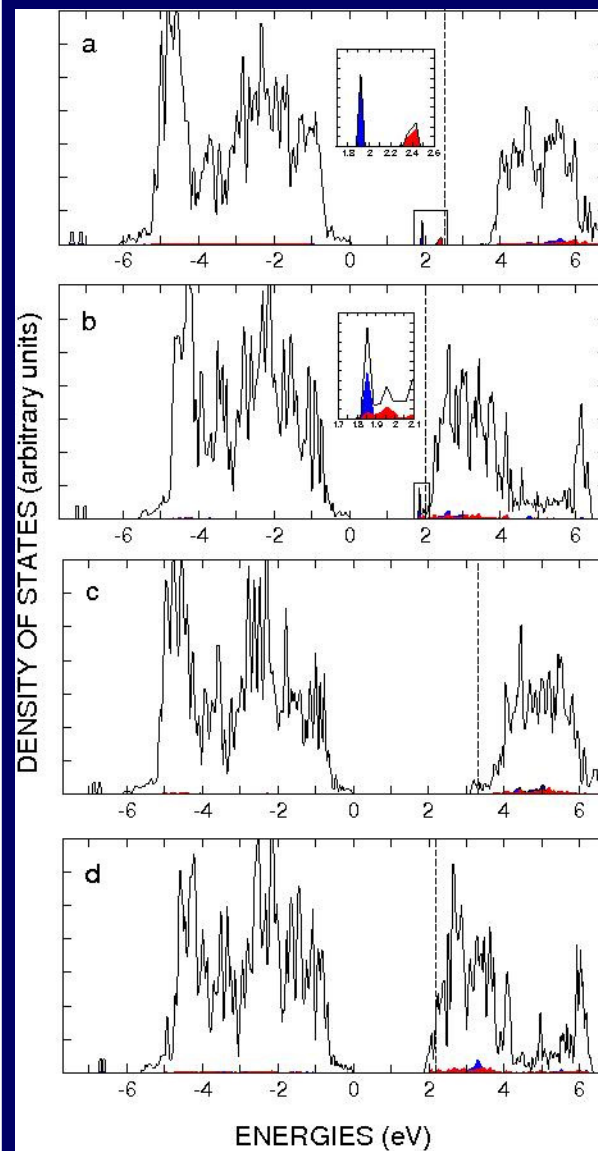
Finazzi, Di Valentin, Selloni, GP, J. Chem. Phys. 128, 182505 (2008)

Polaronic nature of localized Ti^{3+} centers

O vacancy in rutile $TiO_2(110)$: strong distortion around the defect (similar for hydroxylated surface, where Ti^{3+} forms)



Distortion essential to induce localization but present only using hybrid DFT or DFT+U



← Geometry: B3LYP
DOS: B3LYP
localization

← Geometry: B3LYP
DOS: PBE
localization

← Geometry: PBE
DOS: B3LYP
no localization

← Geometry: PBE
DOS: PBE
no localization

THEORY OF TiO₂: THE BAND GAP PROBLEM

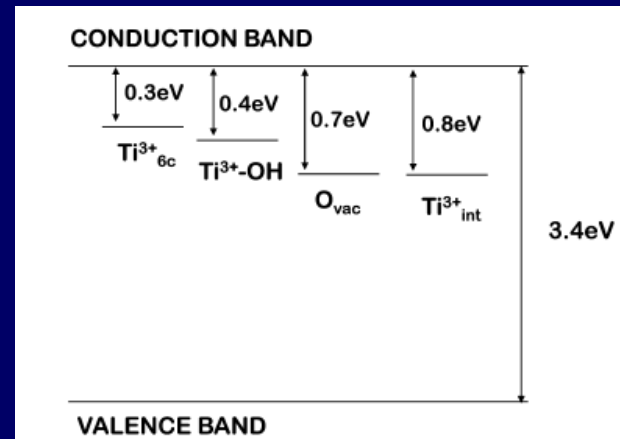
- 1) What is the band gap of anatase TiO₂?
- 2) Optical band gap and direct band gap (from direct and inverse photoemission)
- 3) Excitonic contributions

Exp. (anatase)	3.2-3.4 eV
DFT GGA	2.2-2.6 eV
DFT+U	2.4-2.8 eV
Hybrid functionals	3.5-4.1 eV
GW ^(a)	3.6-3.8 eV

(a) Thulin, Guerra, Phys. Rev. B 77, 195112 (2008); Chiodo et al. Phys. Rev. B 82, 045207 (2010); Kang, Hybertsen, Phys. Rev. B 82, 085203 (2010)

Description of band gap has direct effects on nature of Ti³⁺ states in reduced TiO₂

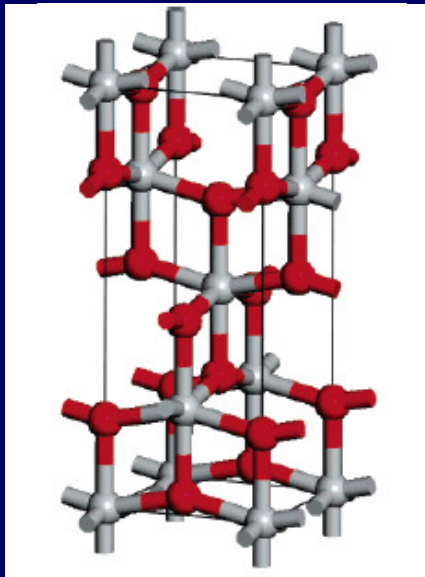
Di Valentin, GP, Selloni, J. Phys. Chem. C 113, 220 (2009)



NITROGEN DOPING OF OXIDES

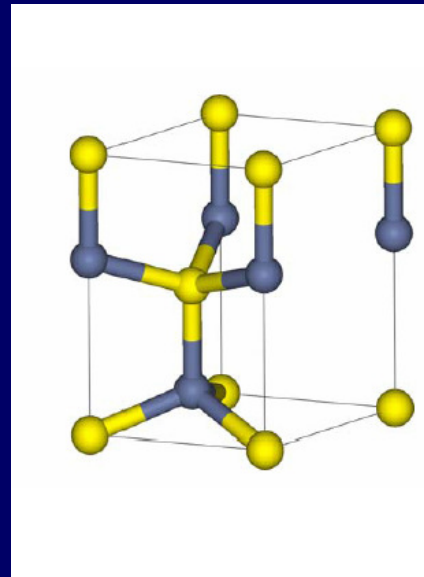
Nitrogen: an important doping element in different oxides

TiO₂
gap 3.2 eV



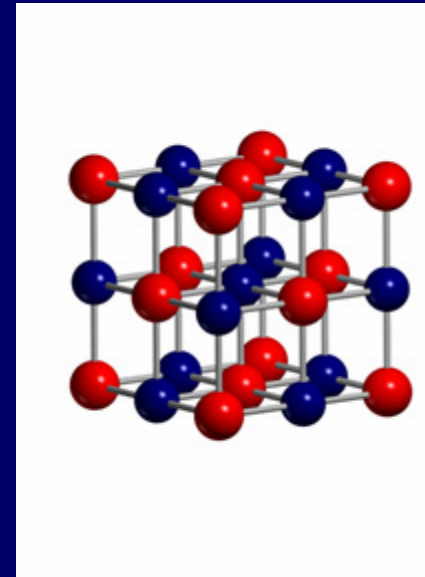
Photocatalysis
Dye-sens. solar cells

ZnO
gap 3.4 eV



Optoelectronics
Photochemistry

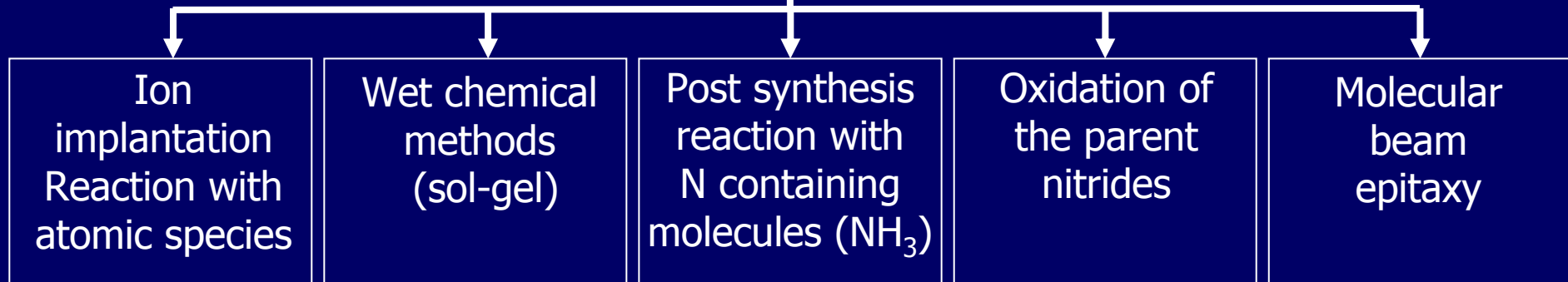
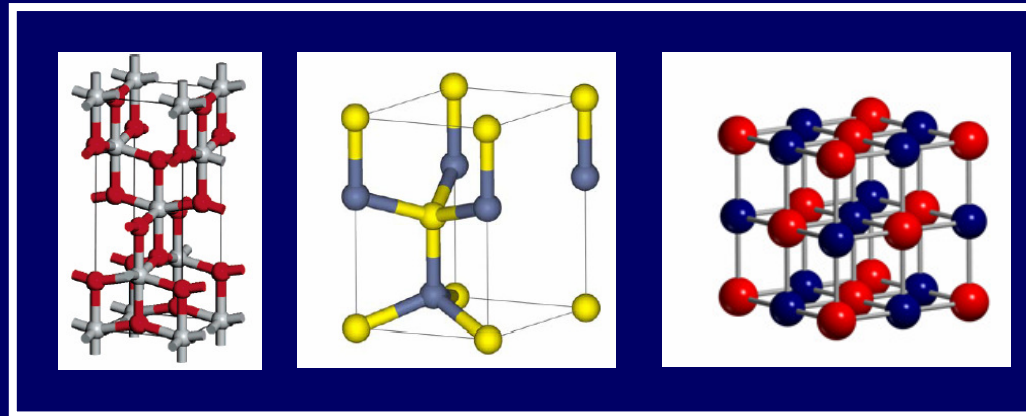
MgO
gap 7.8 eV



Magnetic materials
Spintronics

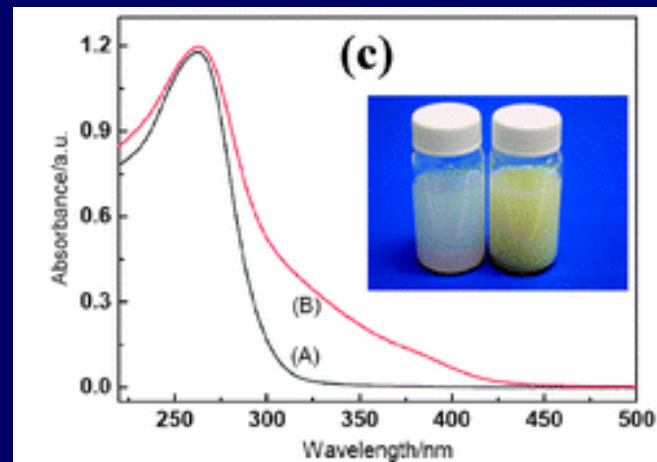
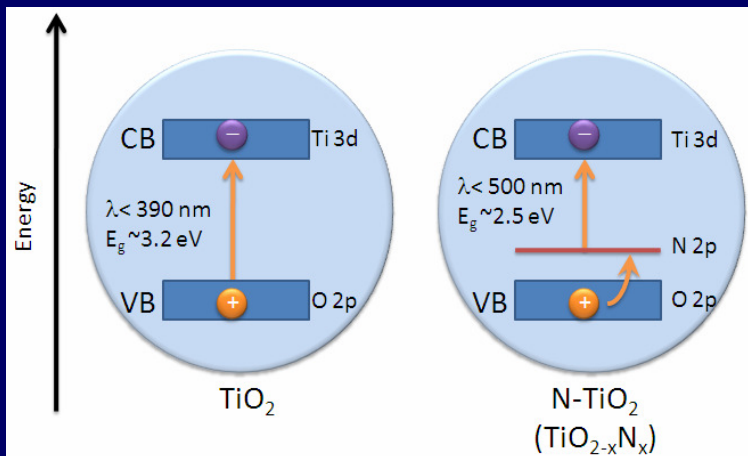
NITROGEN DOPING OF OXIDES

Nitrogen can be introduced in the oxide matrix via different ways



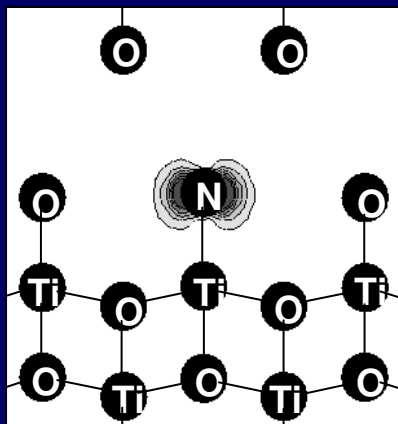
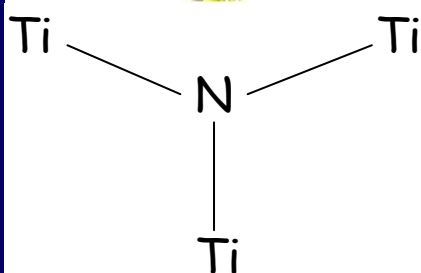
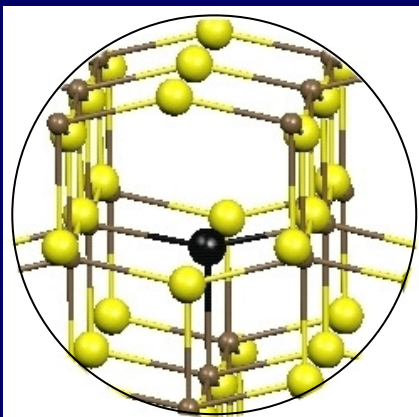
WHY N-DOPED TiO₂ ?

Photocatalyst under visible light

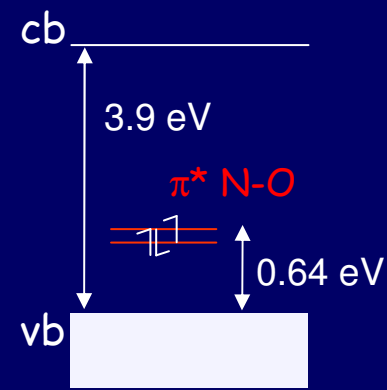
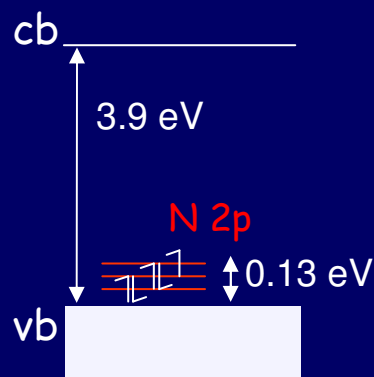
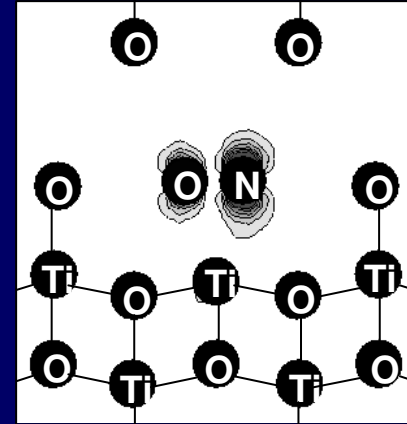
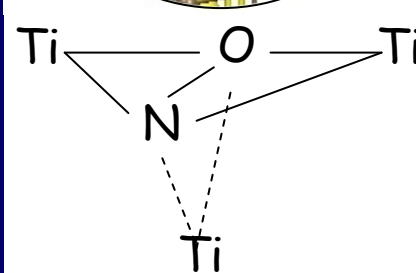
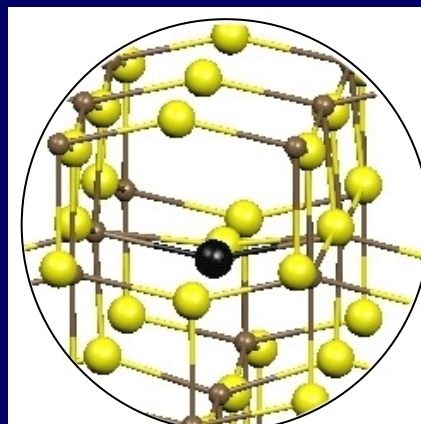


NITROGEN DOPED ANATASE: DFT (B3LYP)

substitutional
Nitrogen N_{sub}



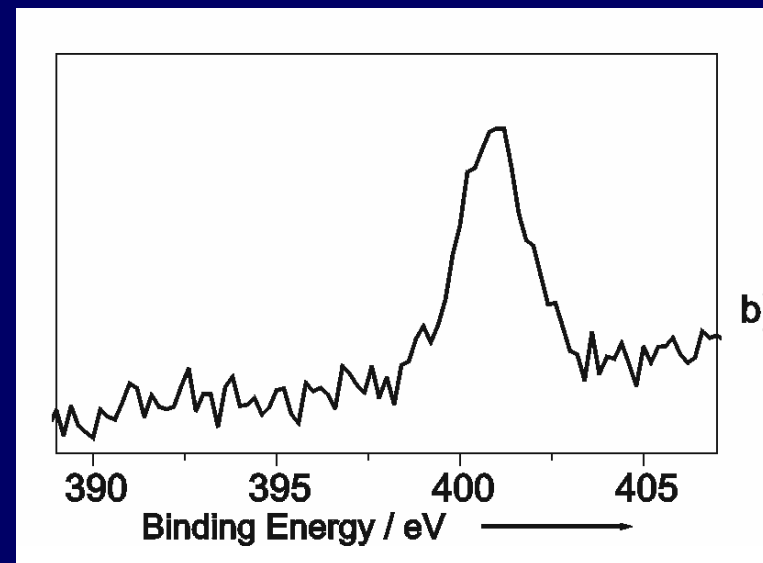
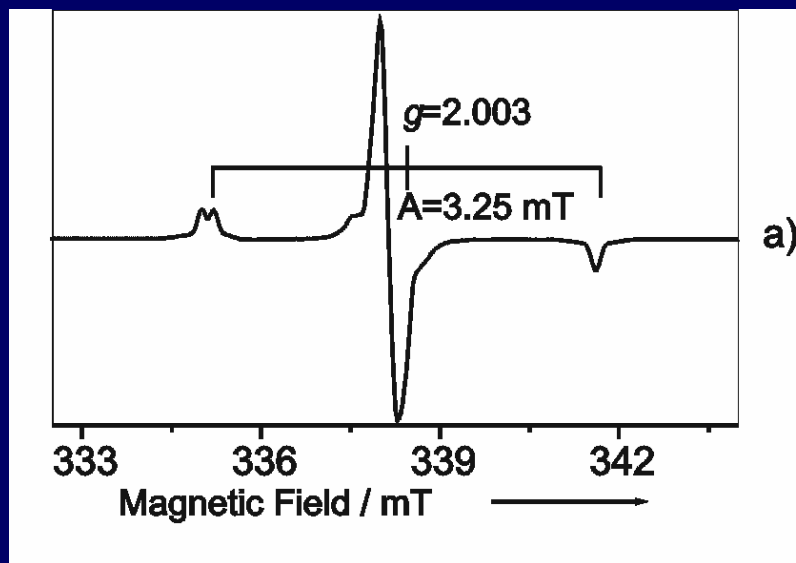
interstitial
Nitrogen N_{int}



Substitutional N (paramagnetic) introduces localized states just above the O 2p valence band

Interstitial N forms a strong N-O bond (kind of paramagnetic NO^{\bullet} molecule); localized states higher in the gap

Substitutional versus interstitial N-doping: EPR and XPS



EPR	a_{iso}	B_1	B_2	B_3
exp	13.0	-10.0	-10.0	20.0
N_{int}	11.8	-11.6	-10.0	21.6
N_{sub}	14.5	-12.0	-11.7	23.7

XPS	N_{sub}	N_{int}
exp	~396	~400-401
Theory	Lower BE	Higher BE

Both hyperfine coupling constants (G) and XPS (eV) indicate formation of interstitial N – Unambiguous identification possible

Napoli, Chiesa, Livraghi, Giamello, Agnoli, Granozzi, Di Valentin, GP, Chem. Phys. Lett., 477, 135 (2009)

WHY N-DOPED ZnO ?

p-type conductivity



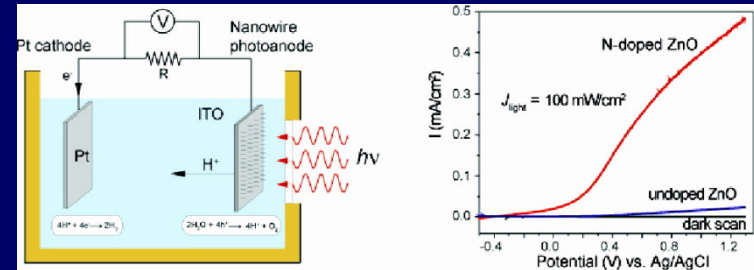
Luminescence of ZnO samples

Main problem for use of ZnO in electro-optic devices is ambipolar doping (e.g. easy n-type and difficult p-type doping)

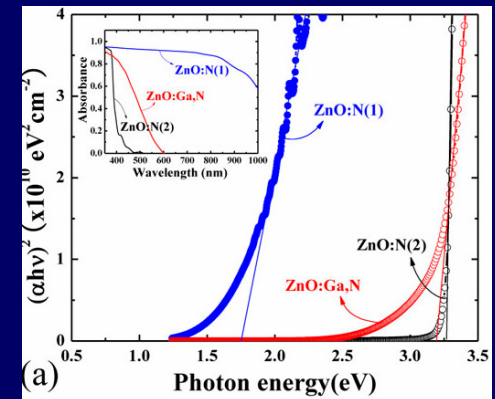
Li (monovalent) good candidate but Li-ZnO does not show p-type conductivity because interstitial Li acts as a donor

N, P, As replacing O are good candidates

Photoanodes in water splitting

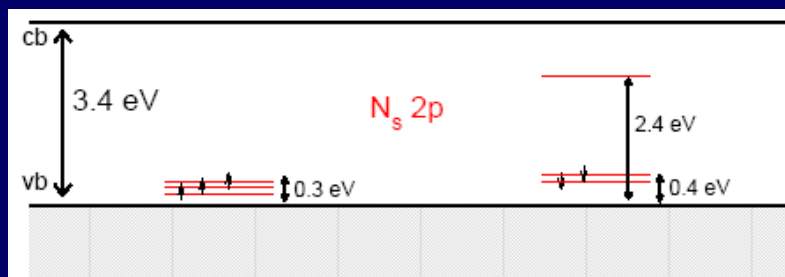
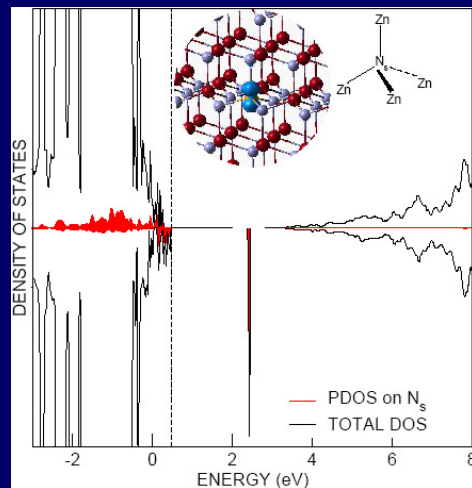


photoanodes in photoelectrochemical cells for hydrogen generation from water splitting



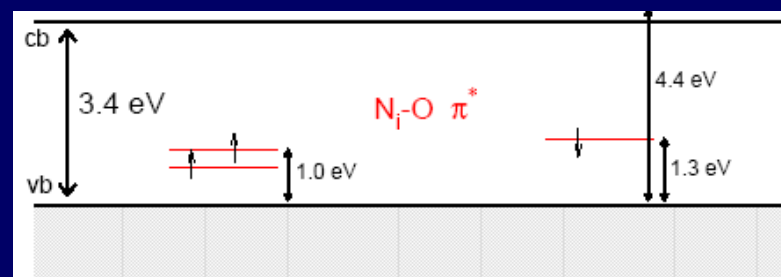
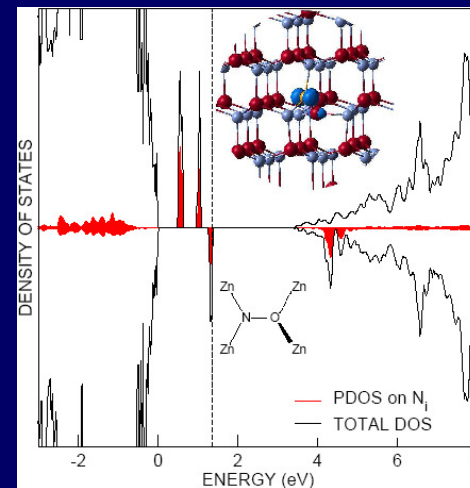
NITROGEN DOPED ZnO: DFT (B3LYP)

Substitutional Nitrogen N_{sub}



Substitutional N (paramagnetic) introduces localized 2p states just above the O 2p valence band

Interstitial Nitrogen N_{int}

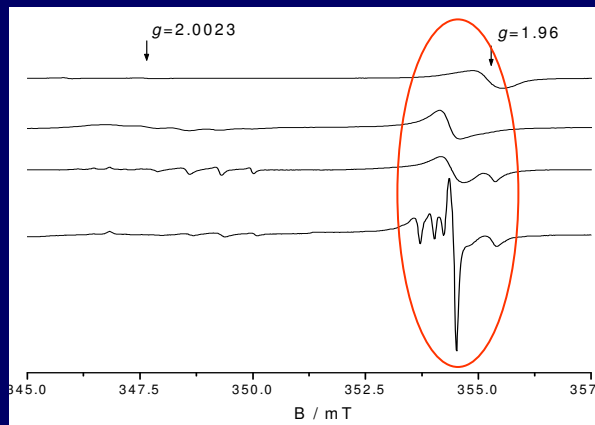


Interstitial N forms a strong N-O bond (kind of paramagnetic NO^* molecule); localized states higher in the gap

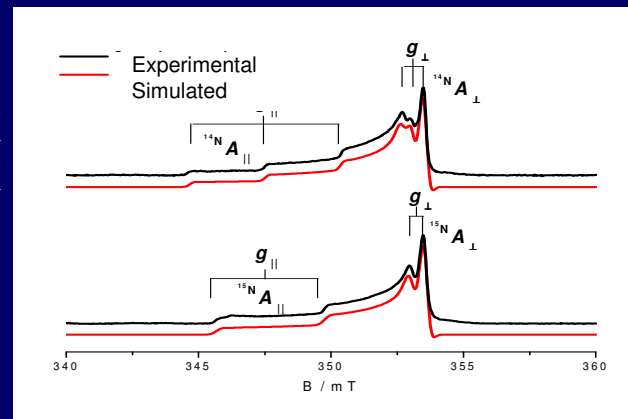
Very similar to N-doped anatase TiO_2

NITROGEN DOPED ZnO: SUBSTITUTIONAL OR INTERSTITIAL?

Annealing under NH_3 atmosphere @650 °C followed by oxidation @500 °C \rightarrow N-ZnO



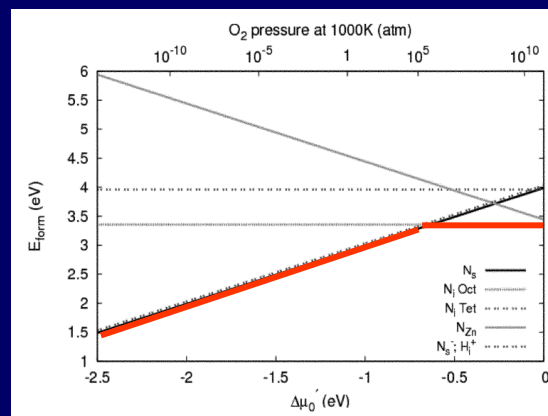
ZnO 77 K
 NH_3/ZnO 77 K
 NH_3/ZnO 20 K
 NH_3/ZnO 4 K



Electron spin echo detected EPR and HYSCORE: hyperfine and quadrupolar tensors

EPR	a_{iso}	B_{xx}	B_{yy}	B_{zz}
exp	7.6	-10.7	-10.7	21.4
N_{sub}	7.0	-11.1	-11.1	22.1
N_{int}	11.0	-13.5	-12.7	26.2

Comparison of DFT with EPR data (G): substitutional N in better agreement



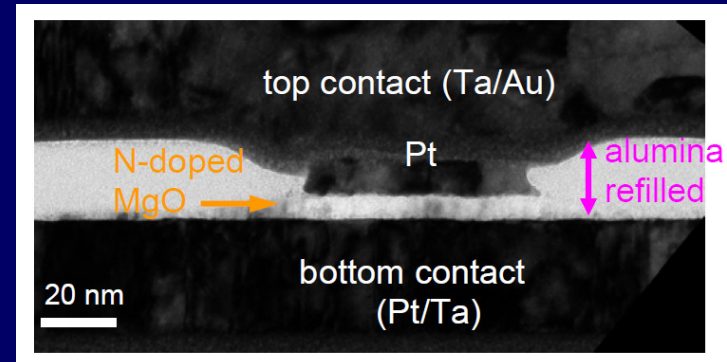
Ab initio thermo-dynamics: substitutional N preferred in a wide range of O chemical potential

Gallino, Di Valentin, GP, Chiesa, Giamello, J. Mater. Chem. 20, 689 (2010)

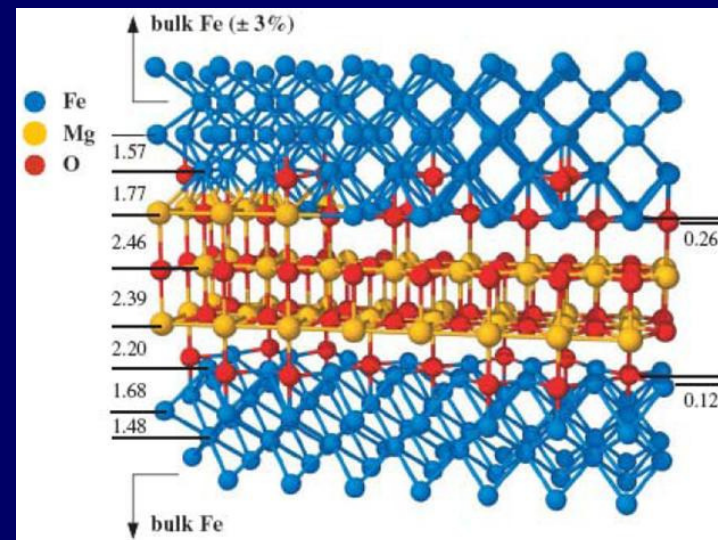
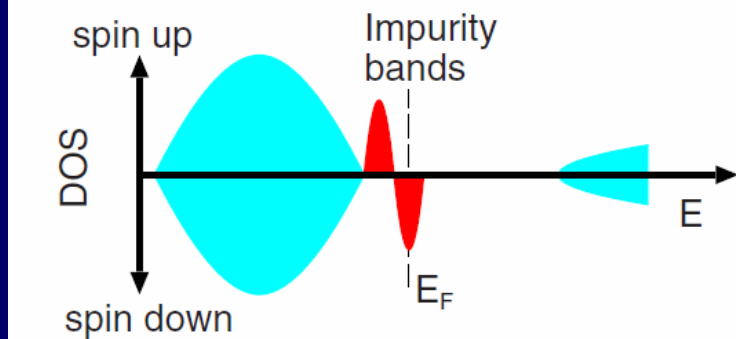
WHY N-DOPED MgO ?

Diluted magnetic insulators

- Transform non-magnetic MgO in RT ferromagnet (d^0 ferromagnetism)
- N-MgO layers exhibit voltage controlled resistance states (a high resistance and a low resistance state). The basis for new resistive switching devices
- New generation of magnetic tunnel junctions



(b) Anion substitution



N-DOPED SrO: PRESENCE OF MAGNETIC IMPURITIES

PRL 98, 137202 (2007)

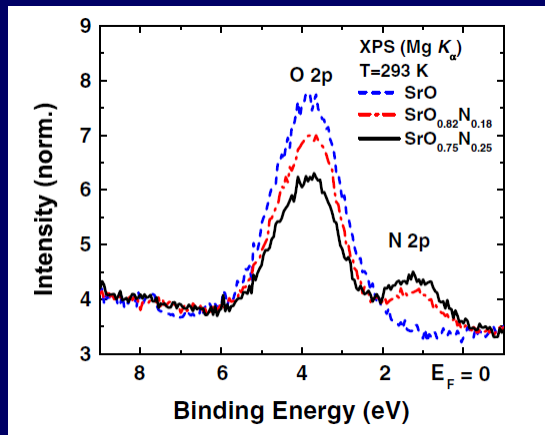
PHYSICAL REVIEW LETTERS

week ending
30 MARCH 2007

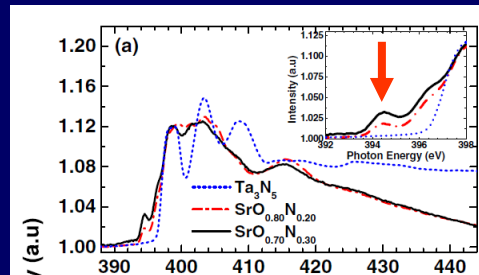
Magnetizing Oxides by Substituting Nitrogen for Oxygen

I. S. Elfimov,¹ A. Ruydi,² S. I. Csiszar,³ Z. Hu,⁴ H. H. Hsieh,⁵ H.-J. Lin,⁵ C. T. Chen,⁵ R. Liang,¹ and G. A. Sawatzky¹

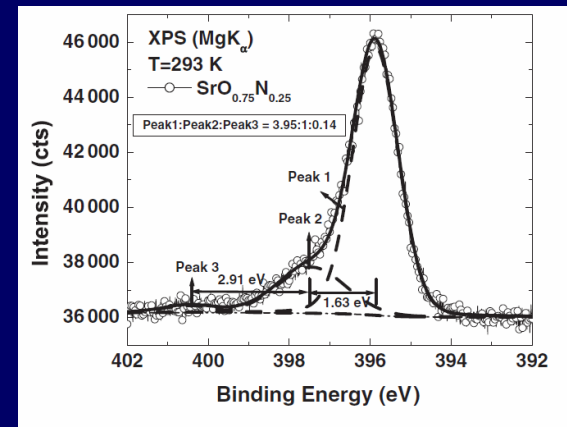
Films of N-doped SrO produced by MBE in UHV (NO as oxidizing agent)



Valence band XPS shows N 2p states above O 2p valence band



XAS: pre-peak at N K edge strongly supports presence of N 2p hole

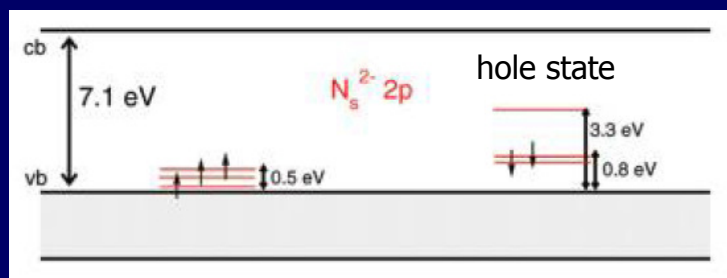
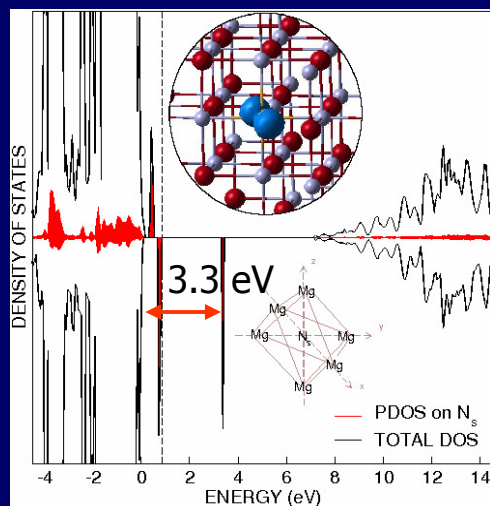


Double peak structure in N 1s XPS indicative of singlet-triplet exchange splitting (N 2p hole)

Alkaline-earth oxides can be doped with N to generate magnetic defects

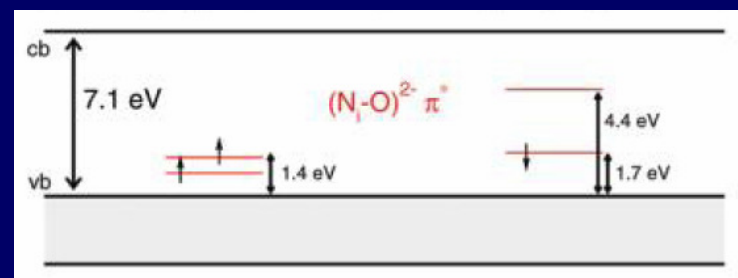
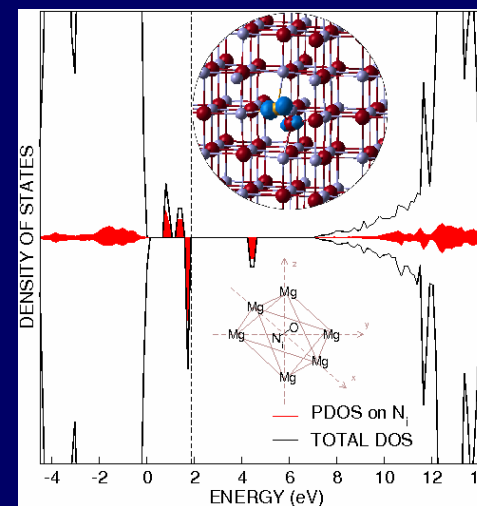
NITROGEN DOPED MgO: DFT (B3LYP)

Substitutional Nitrogen N_{sub}



3% substitutional N (paramagnetic) introduces localized 2p states 0.5-0.8 eV above the O 2p valence band

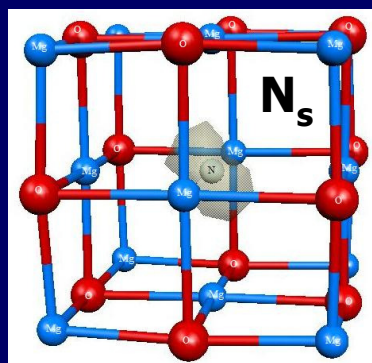
Interstitial Nitrogen N_{int}



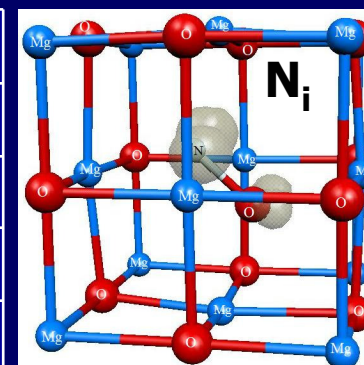
3% interstitial N forms a strong N-O bond (NO^\bullet molecule); localized states in the gap 1.4-1.7 eV above top of VB

Similar to N-doped TiO_2 and ZnO (but much larger gap!)

NITROGEN DOPED MgO: COMPUTED EPR PROPERTIES

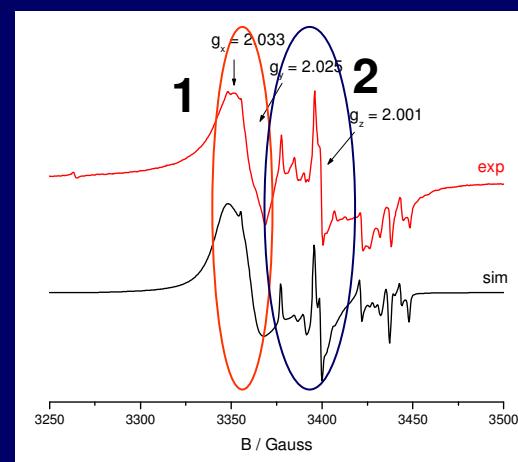
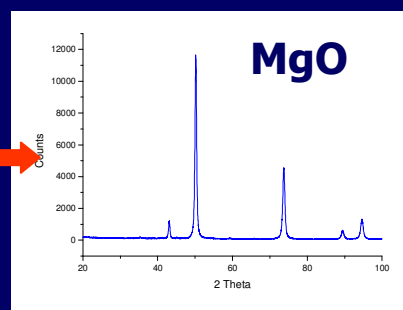
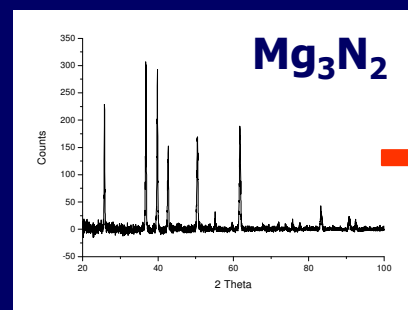


EPR	(G)	a_{iso}	B_1	B_2	B_3
N_s	Periodic	13.6	-11.9	-11.9	23.8
	Cluster	10.8	-10.8	-10.8	21.6
N_i	Periodic	13.0	-11.8	-11.3	23.2
	Cluster	11.1	-10.6	-10.6	20.8



Periodic supercell and embedded cluster calculations: same results
 Substitutonal and interstitial N give very similar hyperfine tensors

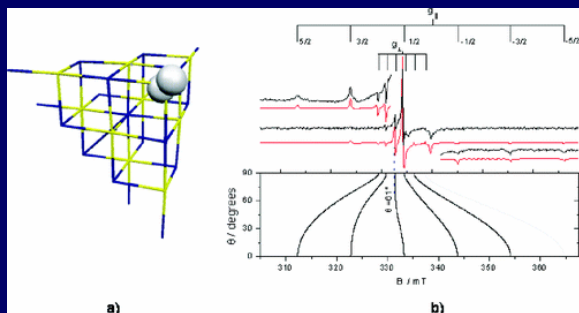
Pesci, Gallino, Di Valentin, GP, J. Phys. Chem. C 114, 1350 (2010)



Prepare N-MgO from oxidation of Mg_3N_2
 @800 °C (Chiesa, Giamello, 2010)

Oxidation of Mg_3N_2 leads to cubic MgO with two kinds of paramagnetic impurities, type 1 and type 2

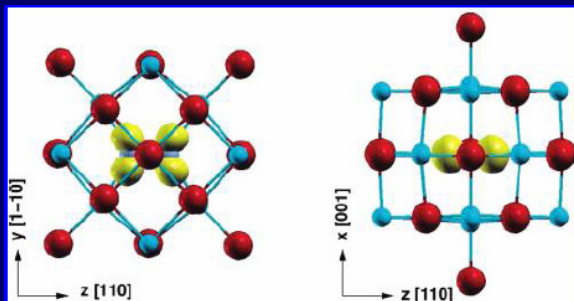
N-DOPED MgO: NATURE OF PARAMAGNETIC SPECIES



TYPE 1 SPECIES: O⁻ IONS

Type 1 species identified as O⁻ radical from comparison with previous spectra

Chiesa, Giamello, Di Valentin, GP, Chem. Phys. Lett. 403, 124 (2005)



TYPE 2 SPECIES: N₂⁻ TRAPPED AT MgO LATTICE

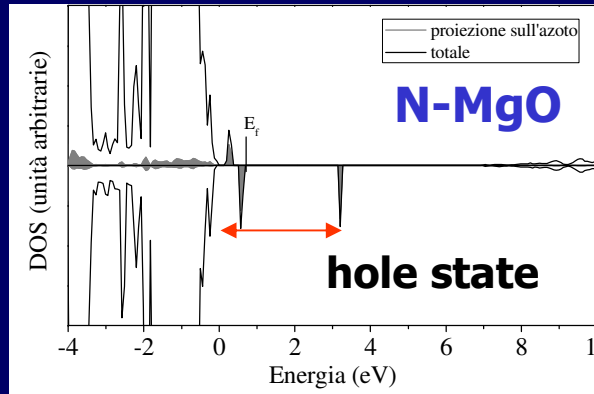
Unambiguous identification of type 2 species as N₂⁻ from comparison of theory and exp.

EPR	g_{xx}	g_{yy}	g_{zz}	a_{iso}	B_{xx}	B_{yy}	B_{zz}
Exp.	2.0043	2.0021	1.9833	4.5	-7.8	17.7	-9.9
Theory	2.0041	2.0023	1.9873	6.4	-8.5	16.7	-8.1

Napoli, Chiesa, Giamello, Fittipaldi, Di Valentin, Gallino, GP J. Phys. Chem. C 114, 5187 (2010)

No presence of N-atom radical species

EVERYTHING CLEAR? THEORY VS EXPERIMENT

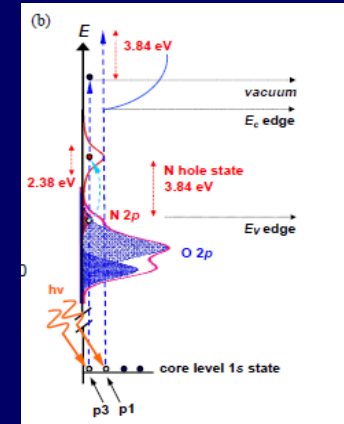


Points of agreement

N 2p occupied states about 0.8 eV above top of VB

Hole in 2p N orbital

Similar position of N hole state in band gap (3.8 eV from top of VB)



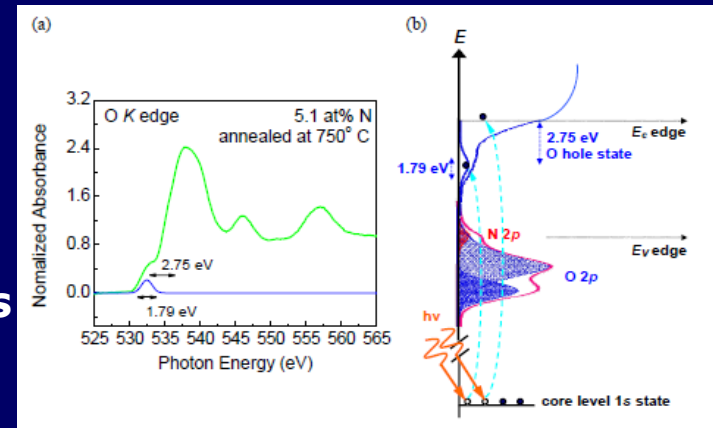
Points of disagreement

Theory: spin pop. on N 0.9 (3% doping)

Exp.: max. moment on N 0.35 μ_B /atom (2% doping)

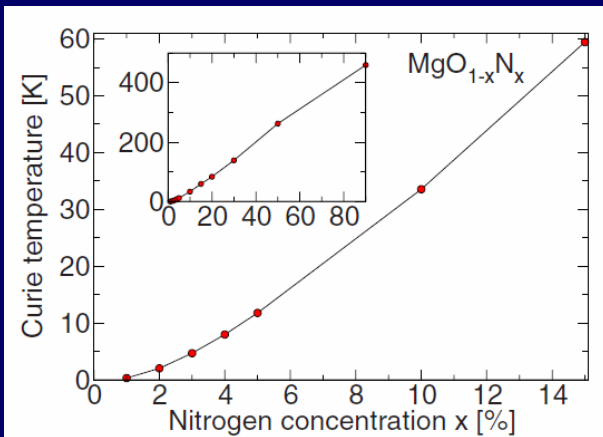
Pre-edge feature in O K edge NEXAFS reveals local unoccupied state (hole) in O 2p state

Not observed in DFT calculations



EPR analysis of N-doped MgO films would be very valuable

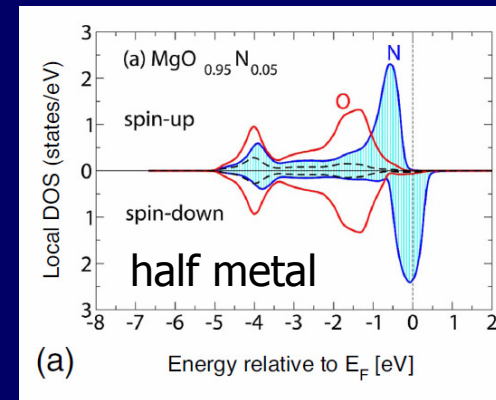
EVERYTHING CLEAR? THEORY VS THEORY



LDA model; T_c from RPA for diluted systems

Mavropoulos, Lezaic, Blügel, Phys. Rev. B 80, 184403 (2009)

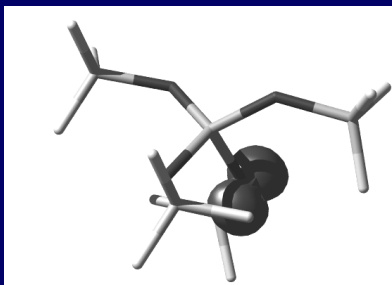
- N-MgO: ferromagnetic (FM) ordering (small $J_{nn'}$ < 10 meV)
- Hole 0.5 on N, rest on 12 neighbors (delocalized)
- Ferromagnetic order via impurity band mechanism
- Limit N concentration for percolation threshold 1.5%



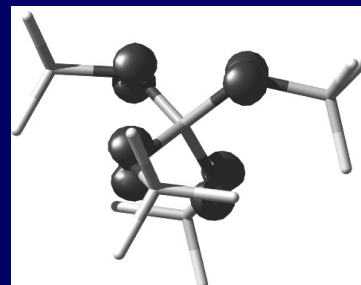
- Limitation in the model: use of LDA
- In LDA N-MgO is half-metal at 5% N doping

Al-SiO₂ (8% Al doping)

Compare magnetic properties from LDA with Self-Interaction-Corrected (SIC) DFT



- SIC DFT: hole localized
- FM and AFM states in Al-SiO₂ separated by 1 meV



- LDA: hole delocalized
- Al-SiO₂, FM state 120 meV more stable than AFM
- magnetic behaviour predicted but never observed

Droghetti, Pemmaraju, Sanvito, Phys. Rev. B 78, 140404 (2008)

HIGHLY DILUTED N-IMPURITY IN TiO_2 , ZnO , MgO

Substitutional Nitrogen N_{sub}

N_{sub}	a_{iso}	B_1	B_2	B_3
TiO_2	14.5	-12.0	-11.7	23.7
ZnO	7.0	-11.1	-11.1	22.1
MgO	13.6	-11.9	-11.9	23.8

Interstitial Nitrogen N_{int}

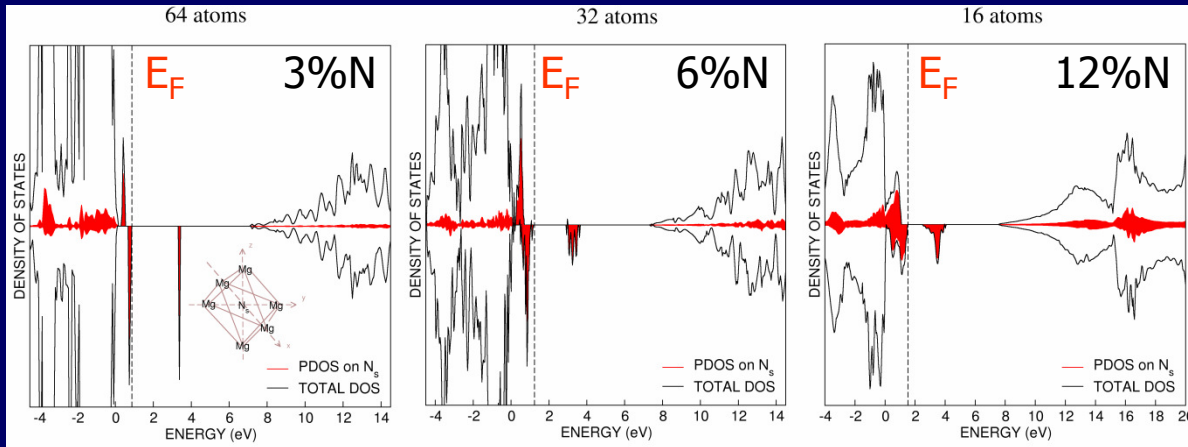
N_{int}	a_{iso}	B_1	B_2	B_3
TiO_2	11.8	-11.6	-10.0	21.6
ZnO	11.0	-13.5	-12.7	26.2
MgO	13.0	-11.8	-11.3	23.2

- Unpaired electron in N 2p (subst.) or a N-O 2π (interstitial) orbitals
- hf tensor independent of electronic/geometrical structure of the host
- where possible (TiO_2 , ZnO) comparison with experiment very accurate
- Physical picture for very diluted N impurities is correct

Unpaired electron on N dopants very localized
Origin of magnetic ordering?

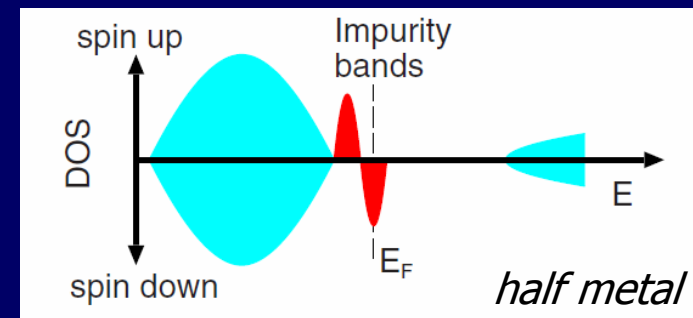
FROM IMPURITY LEVELS TO IMPURITY BANDS

■ N-doped MgO: how properties depend on N concentration?



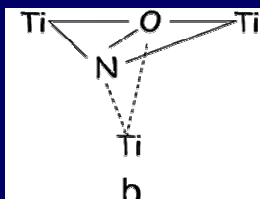
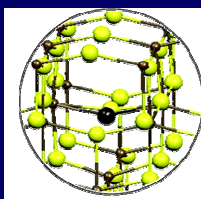
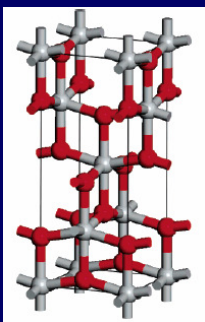
[N]	ΔE (hole- VB)	Band width, W
3%	3.3 eV	0.1 eV
6%	2.5 eV	0.7 eV
12%	1.0 eV	1.5 eV

- Hybrid DFT: even at 12.5% N doping, impurity band is insulating
- $\Delta E(\text{hole state-Valence band}) > \text{band width } (W)$
- Unpaired electron strongly localized, negligible magnetic coupling
- Only mechanism left for magnetic coupling is superexchange (but extremely weak, estimate 1 meV)
- Much larger N concentration needed in order to reach half-metal behavior

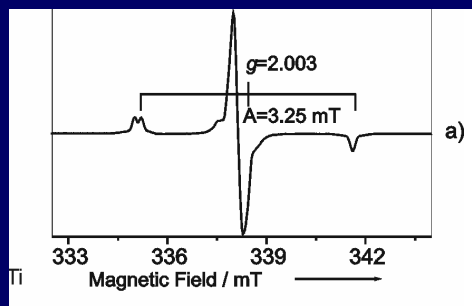


NITROGEN DOPING OF OXIDES: SUMMARY

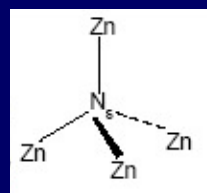
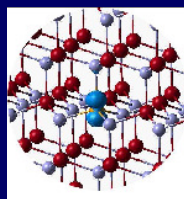
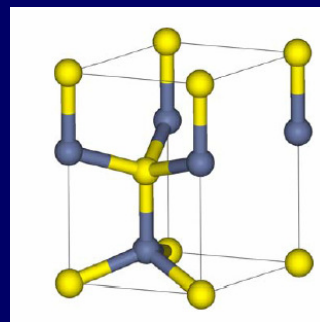
TiO₂



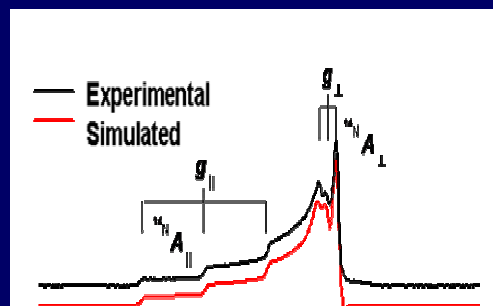
N interstitial



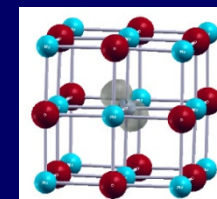
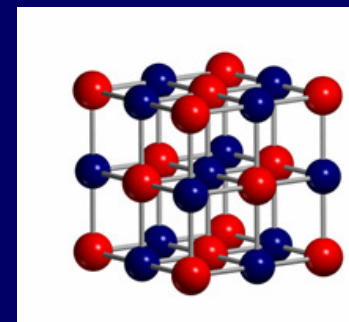
ZnO



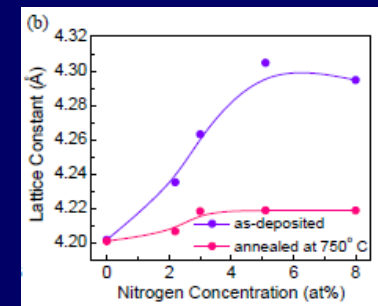
N substitutional



MgO



N substitutional



DILUTED MAGNETIC SEMICONDUCTING OXIDES

Proper treatment of electronic structure (hybrid functionals): very localized magnetic defects, no way to get room temperature ferromagnetism

Incorrect treatment of spin properties (LDA): ferromagnetism predicted for diluted magnetic semiconducting oxides (in agreement with some experimental measurements)

Materials
Views

www.MaterialsViews.com

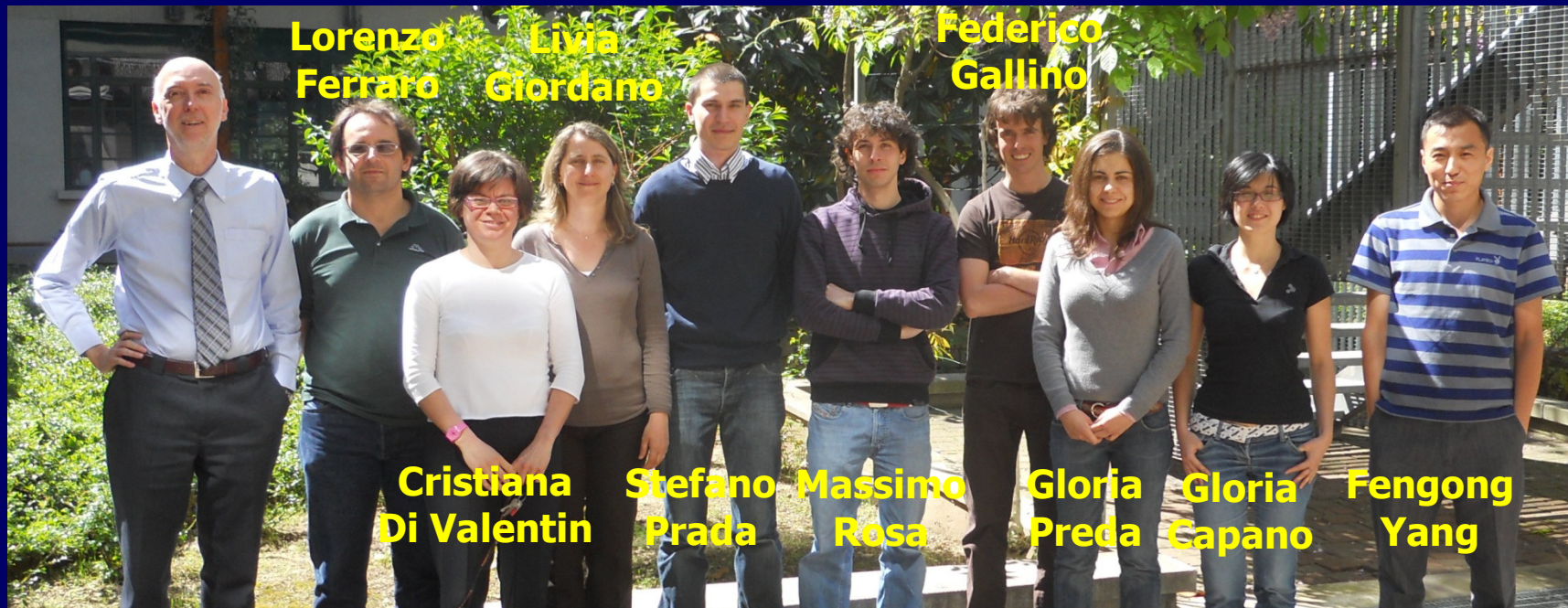
ADVANCED
MATERIALS
www.advmat.de

Dilute Doping, Defects, and Ferromagnetism in Metal Oxide Systems

Adv. Mater. 2010, 22, 3125–3155

By Satishchandra B. Ogale*

Over the past decade intensive research efforts have been carried out by researchers around the globe on exploring the effects of dilute doping of magnetic impurities on the physical properties of functional non-magnetic metal oxides such as TiO_2 and ZnO . This effort is aimed at inducing spin functionality (magnetism, spin polarization) and thereby novel magneto-transport and magneto-optic effects in such oxides. After an early excitement and in spite of some very promising results reported in the literature, this field of diluted magnetic semiconducting oxides (DMSO) has continued to be dogged by concerns regarding uniformity of dopant incorporation, the possibilities of secondary ferromagnetic phases, and contamination issues.



E Giamello



M Chiesa



M Paganini



A. Selloni

Support: MIUR (PRIN 2009, FIRB 2011) – Cariplo – CILEA super-computing Center – COST